Characterization of Water Column Structure in the Northern Andaman Sea, Myanmar based on Field Data collected in December 2017

by:
Jacob Wacht

Courtney K Harris

Advisor: Prof. Courtney Harris

Co-Advisor: Prof. Jeff Nelson

Todd Averett

Senior Coordinator: Prof. Todd Averett

Department of Physics
College of William and Mary
Williamsburg, Virginia
May 2021

Contents

Acknowledgments

I would like to thank Dr. Courtney K. Harris for the help, support, insight, direction, flexibility, and expertise provided to me even before this thesis starting with my REU research during the summer of 2019. Without Dr. Harris this thesis would not be possible and it was a fantastic experience. Secondly, I would like to thank Matt Fair for similar reasons. Matt has always helped me without hesitation and it has been a joy. Jessica M. Côté, PE, Blue Coast Engineering for providing the Matlab code necessary to analyze the data. Dr. Andrea S. Ogston (University of Washington) for aiding in data analysis. Dr. Steve Kuehl (VIMS) and Dr. Danielle Tarpley (USACOE) for taking the data and providing insight to the collection setup and process. Dr. Jeff Nelson for making this possible and providing insight into the logistics of the physics thesis.

List of Figures

Abstract

Ocean circulation and water column velocities within the Northern Andaman Sea are poorly known and understudied. Understanding the flow dynamics within the Northern Andaman Sea is vital for determining the carbon and sediment transport pathways for studies into carbon sequestration, future global warming, and the local shad fishery health. Until recently, knowledge about the velocities of the ocean water within the study area was based on limited observations of highly energetic surface speeds. Little, to nothing, was known about conditions below the water surface. However, ADCP (Acoustic Doppler Current Profiler), and CTD (Conductivity Temperature Depth) data were obtained during a research cruise located in the Northern Andaman Sea, Myanmar in December of 2017. This data, combined with available tidal data, was analyzed to better understand ocean water motion and structure in the region. The ADCP data was collected along transects that varied in depth from 10-80 meters and were geographically spaced around the Ayeyarwady delta mouth, the Gulf of Martaban, and the Bay of Bengal. CTD data was also collected near the ADCP transects. Tides within the Northern Andaman Sea can exceed 3 meters in amplitude and therefore influence water motion drastically; due to their large impact on the system tidal data was used from five different shore stations for data quality control. Analysis was completed by separating the transects into 3 distinct sections: the Gulf of Martaban, Central Ayeyarwady, and Western Ayeyarwady. Each section exhibited unique water column characteristics. The Gulf of Martaban had a strong tidal dependency with high sediment loads during ebb tide. The Central Ayeyarwady had a general westward flow and highly energetic shear layers at depths over 35 m that traveled in a northwestward direction. The Western Ayeyarwady presented general water movement in a northwestward direction.

---

1 Introduction

The connection between rivers and the world's oceans is vital to quantitative studies of carbon flux and sediment transport. Both sediment and carbon are key drivers that influence global warming, ocean acidity, and water quality. Globally, 87% of land connects to the ocean via rivers (Bianchi et al., 2013). River outflow creates an annual total carbon flux of around 1 Pg C (10^{15} grams carbon) (Bianchi et al., 2013). This carbon flux is approximately equal to the net oceanic - atmospheric carbon ex-

change (Bianchi et al., 2013). Similarly, rivers deliver 20 Pg of sediment to the oceans (Meybeck et al., 2003). Not enough is known about whether the transported carbon and sediment are sequestered to the ocean floor or whether they are re-suspended back into the water column (Bianchi et al., 2013). When carbon is reintroduced into the water column it may be exposed to oxygen and then has the ability to contribute to biological growth and productivity or return to the atmosphere (greenhouse gas emission). When buried in the sea floor the surrounding environment is anoxic, and therefore carbon is not exposed to oxygen and this represents a net sink of carbon. Worldwide, it is estimated that 0.45 Pg C is buried annually in coastal sediments, representing about one-half of the riverine output (Bauer et al., 2013). Determining the complex carbon and sediment transport pathways are vital for climate models and future global warming studies. To accomplish this challenging goal, we need to better understand the fluxes from the largest rivers in the world that dominate the output of sediment and carbon into the ocean.

The world's 25 largest rivers output a majority of the global carbon and sediment transported via river discharge. These rivers account for 50% of the freshwater input and 40% of the particulate matter delivered into the oceans (Bianchi et al., 2013). However, anthropogenic effects such as dams, land use change, and dredging are of increasing concern and can fundamentally alter how these rivers and their tributaries function. Damming and shoreline protection create externalities that drastically alter river water volume, flood plain area, suspended sediment content, and outflow into the oceans. Anthroprogenic changes have created problems that include more severe flooding and altered sediment flux. Reduced sediment loads have led to shortages of the material that builds deltas, making them more vulnerable to erosion via wave action, and causing greater vulnerability to relative sea level rise (Syvitski and Saito, 2007).

However, although almost all rivers face human pressure, the Ayeyarwady and Thanlwin rivers, located in Myanmar, are considered two of the last remaining free flowing rivers in Asia (Grill et al., 2019). The Ayeyarwady-Thanlwin river system places third in the world in terms of suspended sediment discharge, producing over 600 MT (Megatons) annually (Kuehl et al., 2019). Additionally, the rivers output 5.7-8.8 MT of organic carbon annually to the coastal ocean, ranking second behind the Amazon Delta (Bird et al., 2008). Unfortunately, very little is known about the system dynamics or the fate of the carbon and sediment once they reach the ocean. Such large unknowns in sediment and carbon fluxes produce uncertainty in climate studies and predictions.

What is known is that the rivers deliver sediment and carbon into the Andaman Sea, which provides vital nutrients to support massive stocks of phytoplankton there. The phytoplankton feed the tropical hilsa shad fishery (Hossain et al., 2020). The shad fishery supports an estimated 500,000 fisherman and 2.5 million people along the supply chain (Hossain et al., 2020). The supply of fish is entirely dependent on phytoplankton stocks, that rely on nutrients from river outflow, for food availability. Determining the carbon and sediment transport pathways is vital for assessing the health of the shad fishery and maintaining a productive, non-threatened fishery.

The phytoplankton are more than fish feed, on a global scale, the phototrophic organisms fix 30-50 billion metric tons of carbon, about half of the global total (Hossain et al., 2020). Fixed carbon is important due to the fact the carbon is converted from inorganic form CO_2, a greenhouse gas, into organic form that can be sequestered within living cells. To grow phytoplankton require the nutrients provided by the outflows from the Ayeyarwady and Thanlwin river systems. Understanding the fate of carbon and sediments once delivered to the Andaman sea is vital to figuring out when phytoplankton blooms will occur and sequester carbon out of the atmosphere.

However, understanding the water circulation is key to understanding the carbon pathways in the coastal ocean. Particulate carbon travels with sediment which in turn travels as suspended matter along with currents, tides, and waves. Little is known about the transport pathways within the study area.

2 Study Site

2.1 Riverine Background

The Ayeyarwady-Thanlwin river system, displayed in Fig. 1, originates in the eastern Himalayas and flows southward through Myanmar. The region is located on the boundary between the Indian and Eurasian tectonic plates. The overlapping plates helped influence the formation of the Ayeyarwady delta. The low-lying area was home to around 13 million people in 1997 (Hedley et al., 2010), is prone to significant flooding, and vulnerable to relative sea level rise (Liu et al., 2020). With future plans to dam the river, it is vital to develop a comprehensive understanding of how the sedimentary system behaves and how it will respond to alterations in the future.

Both rivers span over 2000 km and have similar catchment areas of 410×10^3 km^2 for the Ayeyarwady and 324×10^3 km^2 for the Thanlwin. Together they drain about 83% of Mayanmar and discharge about 600 MT of sediment (Robinson et al., 2007). A large majority of river discharge takes place during southwest monsoon season that starts in May and ends in October. During that season the area receives more than 1.5 meters of rain, which totals to about 90% of its annual precipitation (Zaw and Wittenberg, 2015). Glacial melt also occurs during the summer months adding to the river discharge (Zaw and Wittenberg, 2015). During the remaining months rainfall decreases drastically and in turn so does river discharge (Zaw and Wittenberg, 2015).

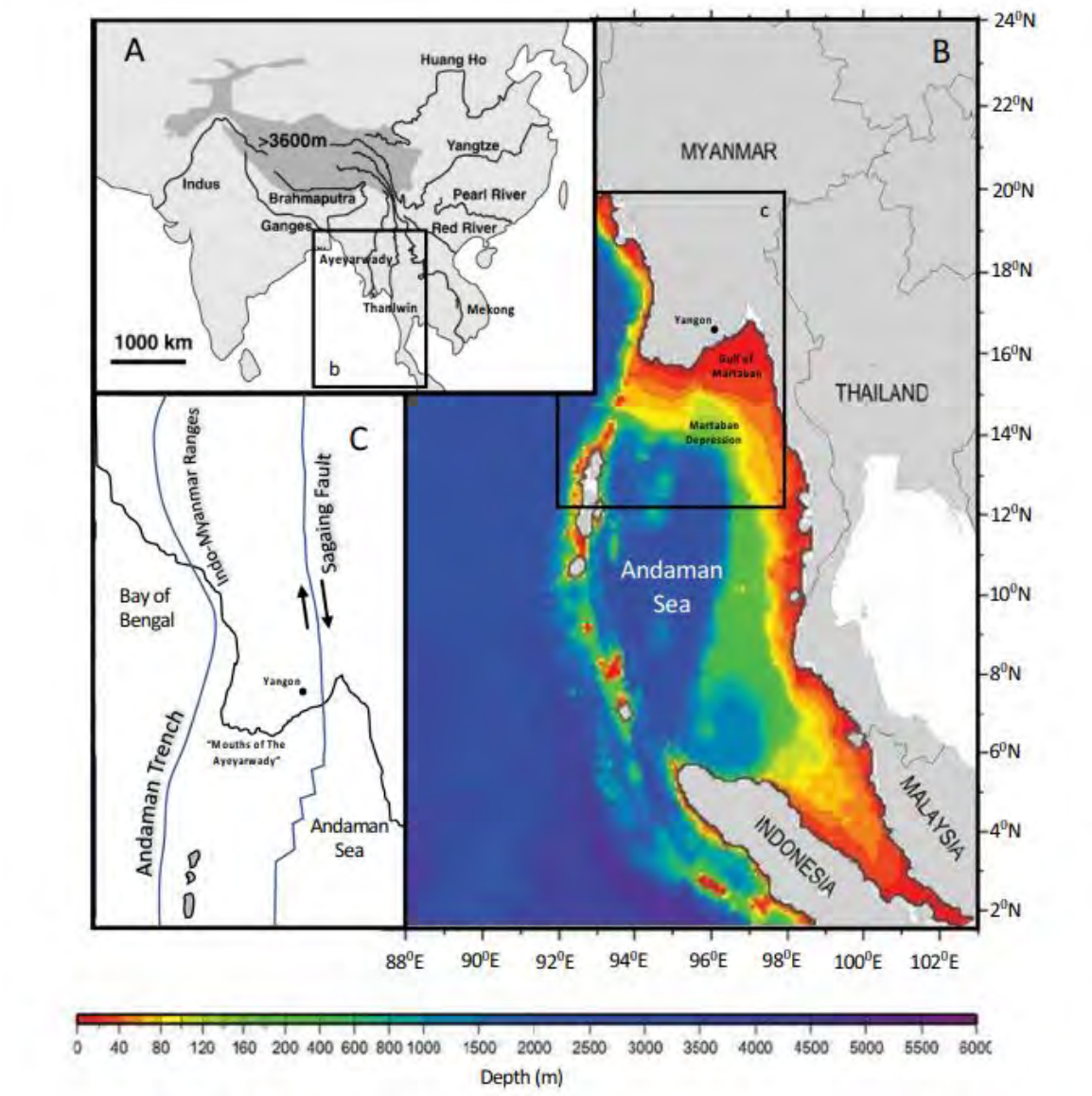

Figure 1: Maps showing the Northern Andaman Sea. Panel (A) highlights the Ayeyarwady and Thanlwin rivers and (B) the Andaman Sea, Gulf of Martaban, and Ayeyarwady river delta courtesy of Kuehl et al. (2019).

2.2 Ayeyarwady Delta

The Ayeyarwady Delta is a tidally-dominated mud slit system that extends about 300 km upstream of the Ayeyarwady River (Hedley et al., 2010). The low-lying river delta is often inundated by tropical cyclones. Its coastal area has a mean tidal range

of about 4 m (Hedley et al., 2010). Little is known about the outflow dynamics within the coastal ocean offshore of the river channels.

2.3 Andaman Sea

The Andaman Sea, mapped in Fig. 1B, has an area of about 800 square kilometers and is bounded by the Bay of Bengal to the west, Ayeyarwady Delta to the north, and land mass consisting of Myanmar, Thailand, and Malaysia to the east. The northeastern Andaman Sea includes the Gulf of Martaban, a funnel shaped embayment located east of the Ayeyarwady Delta. Due to long term sediment output from the Ayeyarwady delta, the northern Andaman Sea has a broad continental shelf about 170 km wide with a steep continental slope at the edge of the shelf (Liu et al., 2020). Like the river discharge discussed above, the continental shelf dynamics are also heavily dominated by seasonal monsoons that alter wind, wave, tidal, and coastal currents (Ramaswamy et al., 2004). From the months May to September the region experiences monsoons with winds from the southwest (southwest monsoon conditions). Wind speeds average 30 km/h during these months. The water velocities at the coastal ocean's surface (surface circulation) are thought to be cyclonic during this season, flowing from the Bay of Bengal with an eastward velocity into the northern Andaman Sea then flowing southward along the eastern boundary (Liu et al., 2020). This creates large pockets of low salinity (less than 20%) water that accumulate on the surface of the Andaman Sea (Liu et al., 2020). During the months December through February, the area experiences monsoons with winds from the northeast having speeds of 15-29 km/h (northeast monsoon conditions) (Liu et al., 2020). This is thought to drive a westward surface flow from the northern Andaman sea into the Bay of Bengal. However, the data supporting the oceanic circulation patterns that result from monsoonal winds is over 60 years old and limited to surface measurements from ship drift (Rodolfo, 1969).

Recent numerical models have indicated that the conditions on a seasonal average follow that general model (Chatterjee et al., 2017). However, on smaller timescales ocean current velocities fluctuate and deviate from the mean. Additionally, numerical models suggest that the near-bed bottom currents that control sediment transport are different from the currents at the ocean surface.

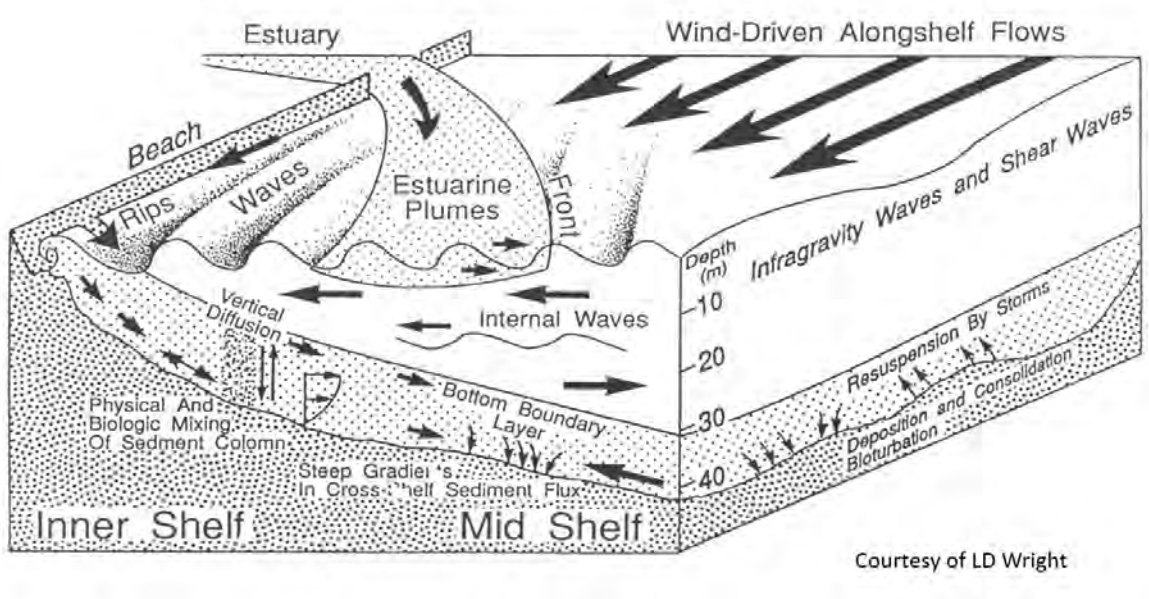

Figure 2: Displays the complex coastal system and sediment transport pathways that impact continental shelves. Said pathways respond to wind, waves, tides, river plumes, storm surges, and more. Courtesy of Wright (1995).

3 Physical Oceanography

Understanding the circulation patterns within the northern Andaman Sea requires that we consider the physical oceanography that is important in that region. This section reviews the basic physical oceanographic theories that have been used to describe and quantify coastal ocean circulation and hydrodynamics. In the coastal zone, ocean circulation responds to tidal forces, pressure gradients, densities, freshwater input, rain, winds, waves, currents, and bottom topography. Therefore, to describe ocean

conditions responsible for carbon and sediment transport requires that we consider those factors and more. Figure 2 illustrates the primary drivers of ocean circulation within an idealized coastal zone, showing how each of those factors are important for the hydrodynamics and sediment transport.

Shifting to the Andaman Sea, in order to better understand the dispersal of sediment and carbon offshore of the Ayeryarwady and Thanlwin Rivers, it is helpful to consider some physical oceanographic concepts that control ocean currents. The concepts include: tides, wind, upwelling, downwelling, and stratification. For example, in the coastal ocean, strong wind forcing tends to drive strong ocean currents that flow parallel to the shoreline. When freshwater empties into the coastal ocean, it tends to remain on the surface due to its decreased density, and can be deflected by the along-coast currents, winds, and/or Coriolis. Both the strong currents and waves can resuspend sediment, which tends to be carried as suspended load in the bottom boundary layer of the coastal ocean. Our understanding of these processes for the northern Andaman Sea has been limited due in part to the lack of observational data there.

3.1 Tides

3.1.1 Theory

Tides are driven by the gravitational forces between the Earth, Moon, Sun (other planets have gravitational forces but are too small for consideration) and the centrifugal acceleration of the earth. The tides create fluctuations in water depth, that are quantified in terms of tidal height (defined as the difference between a water level and the "average" water level often called Mean Sea Level) and tidal range (defined as the difference between the highest and lowest water level over a tidal cycle). The tidal amplitude refers to one-half of the tidal range; that is the difference between

the highest water level and Mean Sea level. Conceptually, as shown in Figure 3, one might assume that the Moon's gravitational force would pull a bulge of water to a single side of the earth.

In reality, this is not the case, due to the Earth's rotation and resulting angular velocity that acts in conjunction with the gravitational forces acting on the oceans (Taylor and Taylor, 2005). A double bulge is created by the change in gravitational force experienced on opposite sides of the earth and the Earth's centrifugal force pushing the oceans away from the rotational axis. On the side of the Earth closest to the Moon, the Moon's gravity dominates and pulls the oceans towards it. On the side of the Earth farther away from the Moon, the centrifugal force opposes and dominates the Moon's gravitational effect. Therefore, a double bulge is created dominated by the Moon, Sun, and Earth's centrifugal force. The tides follow the lunar cycle and are controlled daily by the Moon's position relative to the Earth which leads to two high and two low tides per day at most locations in the ocean and along the coast. The lunar control results in a tidal cycle that is about 13 hours long from high tide to high tide.

The position of the Moon relative to the Sun influence tidal heights as they revolve around the Earth over monthly timescales, and cause tidal range to also vary over these timescales at many coastal locations. The spring tidal phase tidal range is the largest over the lunar month, having higher high tides and lower low tides. During the neap tidal phase, the tidal range is reduced because there are lower high tides and higher low tides. The positions of the Moon that correspond to these times are shown in Figure 4. The phases transition between spring and neap tides every 14 days following the Moon's orbits.

The simplified tidal explanation in Section 5.1 does not take into account the Earth's topography. The Earth's coastal terrain can influence tidal heights and energy

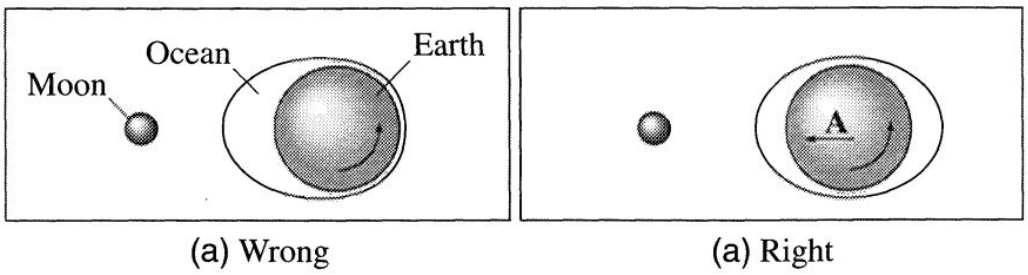

Figure 3: Displays the incorrect (left) and correct (right) assumption about the Earth's tides in relation to the Moon. The double bulge results in the semi-diurnal (two high tides and two low tides per day) tidal cycle experienced in most locations including Myanmar. Courtesy of Taylor and Taylor (2005).

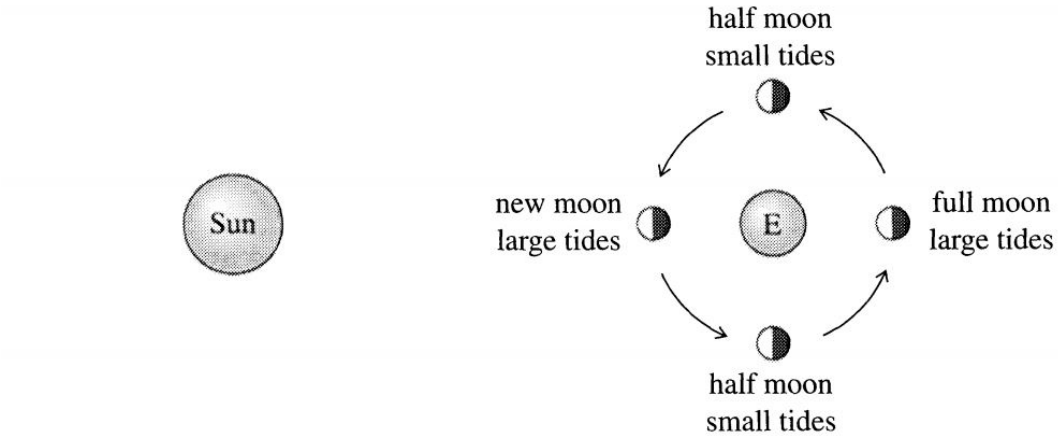

Figure 4: The Moons' positions relative to the Earth and Sun that creates the spring and neap tidal cycle. When the Moon and Sun align, the tidal ranges are at their largest, creating the spring tide. In contrast, when the Moon and Sun are at perpendicular axes to the Earth, tidal ranges are reduced, creating the neap tide as the gravitational forces of the Moon and Sun oppose each other. Courtesy of Taylor and Taylor (2005).

by acting as a funnel. Topography and bathymetry shape the cross-sectional area through which a tidal wave can flow. For example, in the open ocean tides are not constricted, but closer to shore the topography and bathymetry has a large effect.

Tides are often amplified in estuaries and deltas as a result of the land constricting the coastline inward. As a result of the decrease in water depth, the sea floor imparts

a frictional force on the tidal wave that it did not feel in the open ocean. The force causes the amplitude of the tidal wave to increase as a means to satisfy the conservation of energy (Knauss, 1997). An increase in wave amplitude also results when the tidal wave propagates into an inlet or embayment. The constriction means that there is less room to accommodate the discharge. So, the fluid deepens and water velocity may increase to accommodate the volume. The increase in velocity follows Bernoulli's principal which shows that as the cross-sectional area of a flow deceases, flow velocity must also increase.

3.1.2 Tides in the Andaman Sea

These types of topographical features play a role in the tidal phase and amplitude within the northern Andaman Sea. The funneling effect is instrumental to how the tides function in the Andaman Sea, specifically in the Gulf of Martaban. In Figure 10 notice how the Gulf of Martaban narrows as one heads northward. Similarly, the bottom bathymetry also rises steeply from over 400 meters deep to under 40 meters deep. The drastic reduction in width and depth decrease the cross sectional area for the water to flow, which in turn amplifies the tidal speeds and heights in the Gulf of Martaban. As the tide floods the Gulf of Martaban the volume of water pulled by the moon remains constant, but the coastline restricts the width and depth available to the flow. Following the conservation of mass, one can imagine the tide having almost no bounds in the central Andaman Sea, but when the tidal wave reaches the Gulf of Martaban it is now heavily constricted. The decreased flow area increases tidal amplitude and water velocity.

In turn, tides within the Gulf of Martaban (Eastern side of the study area see Fig. 10 and Fig. 6) reach over 3 meters in amplitude. Whereas tides in the region fronting the Ayeyarwady Delta (Western side of the study area: Fig. 10 and Fig. 6)

range only from around 1 to 2 meters in amplitude. This drastic change in height and energy, separated geographically by tens of kilometers, is vital when modeling and understanding how the system functions as a whole.

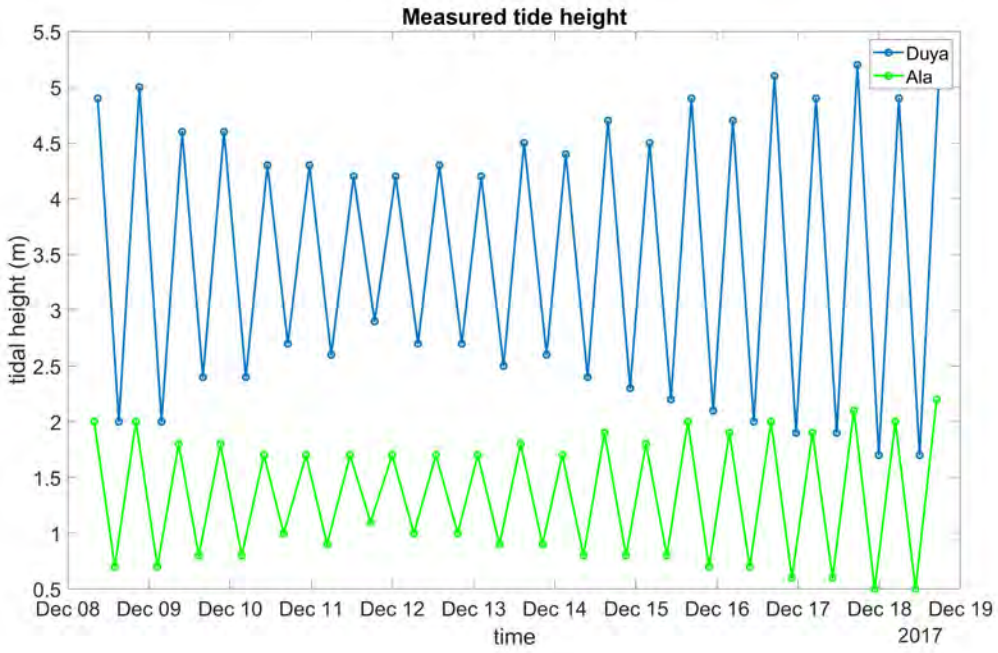

Figure 5: Shows the water levels at the Duya tidal station and the Alandaing station (See Fig. 10 for geographic locations.). The stations are located on opposites sides of the study area and had very different tidal conditions. However, both followed the same spring/neap tidal cycles. The spring tides are present from Dec. 08 to 09 and transition to neap, with neap occurring Dec. 12. The transition is demonstrated by the decrease in amplitude. There is another transition to spring tide phase after the neap. The tides return to their strongest around Dec. 17. Tides had a higher amplitude and change in tide height at the Duya station located in the Gulf of Martaban in comparison with Alandaing (0.75 m) located on the Ayeyarwady Delta.

3.2 Mixing and Stratification

Stratification refers to the way that water density changes with depth in a vertical water column. Well mixed, "stably-stratified", and unstable refer to the way that density changes with depth; with well mixed meaning small changes in density with depth, stable stratification meaning that the denser water underlies less dense water,

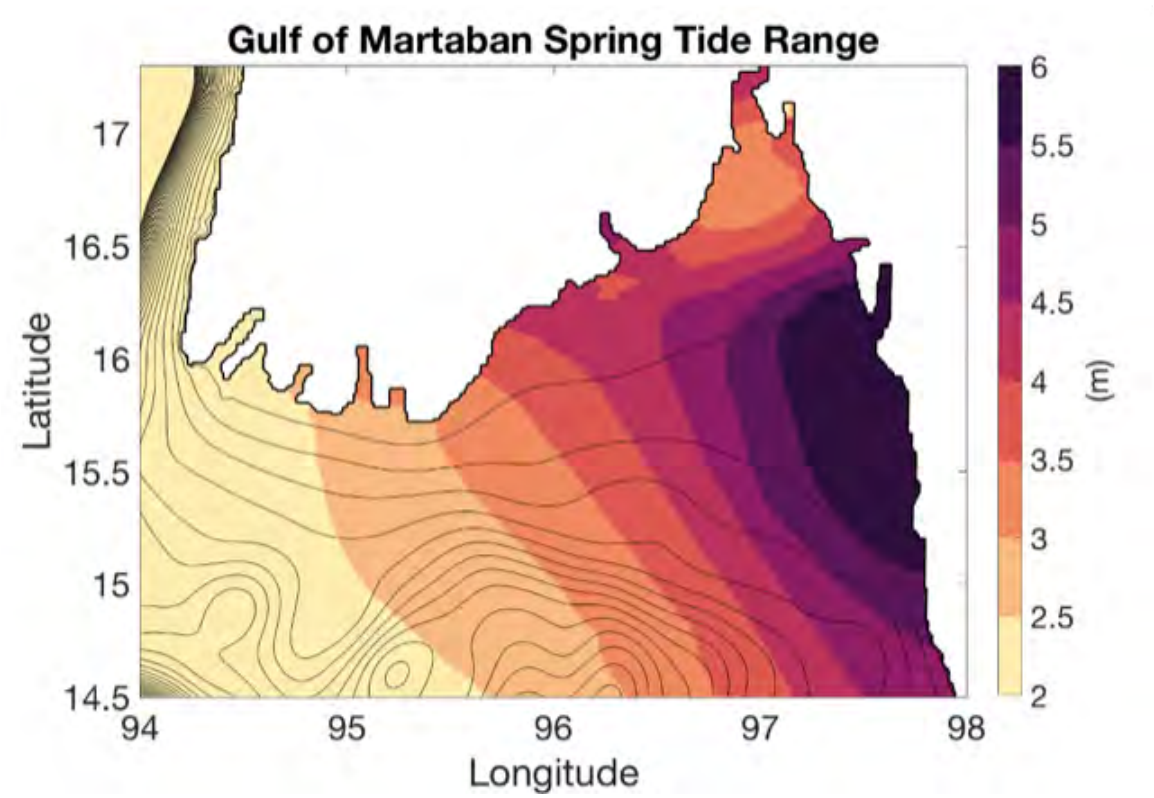

Figure 6: Shows the tidal range modeled within the Northern Andaman Sea. Tidal range increases from west to east to over 6 m in the eastern edge of the study area. This gradient results in vastly changing water conditions and currents. Courtesy of Matt Fair (VIMS).

and unstable stratification referring to the (relatively rare) case of density decreasing with depth. The water column is shown with a 2D sectional view in Fig. 7. This view slices the ocean from the surface to the bottom (Depth on the Z axis). The section reveals water layers with different characteristics tracked by salinity, temperature, suspended sediment concentration, primary productivity, and more. Each unique layer is identified as a parcel, or body of water within the ocean containing similar characteristics. The key to each parcel is they have different densities due to the variations noted above. More salt, lower temperature, and more suspended sediment all result in increased water density (Knauss, 1997).

An easy way to visualize the parcels is by examining Fig. 2, which displays the

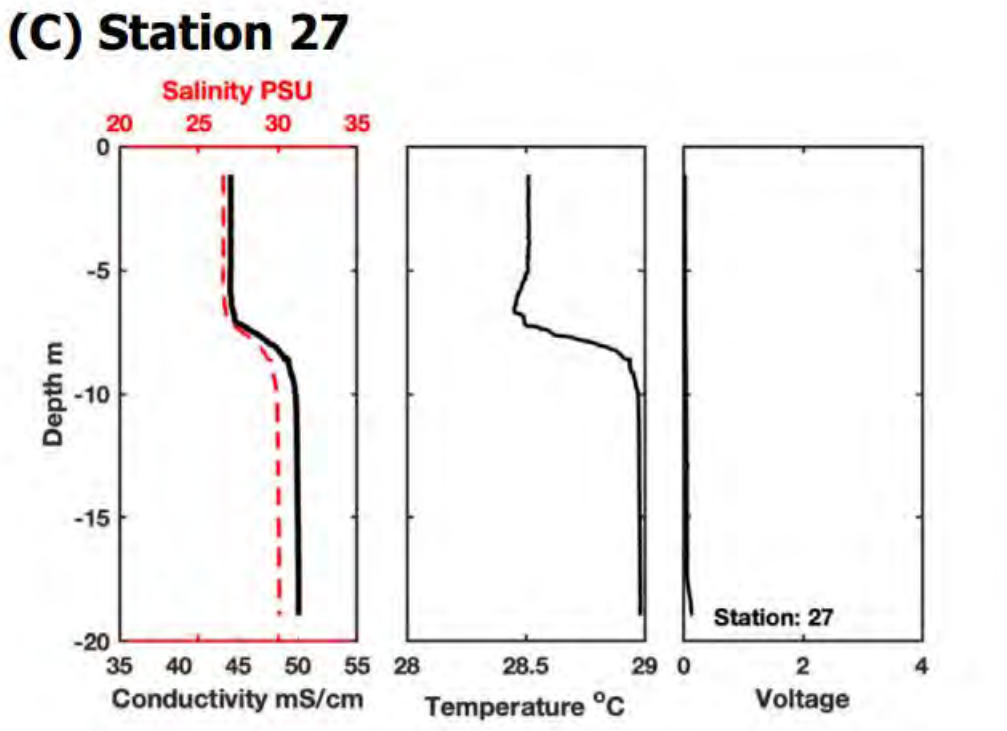

Figure 7: Illustrates an example of a 2D sectional view measured via CTD on the same cruise that the ADCP data was collected. The station 27 showed sharp increases in salinity (PSU) and conductivity (mS/cm) at around 8 m suggesting two separate parcels. This separation is further indicated by the sharp increase in temperature at 8 m. Courtesy of Kuehl et al. (2019).

coastal zone. The vertical panes represent a section view. In those views there are unique features: a freshwater plume due to river output is at the surface and the bottom boundary layer may have increased density as it may be colder and more turbid. Internal waves (See Fig. 2) refer to wave-like oscillations at the boundary layer between parcels having different densities.

A well-mixed water column has very little change in density with respect to depth (Knauss, 1997). Well-mixed water columns generally have intense wind, wave, and tidal action that churn the denser parcels with less dense parcels.

The most common situation is "stable stratification" where less dense water overlays more dense water. The water column is stable when parcels that are less dense

are located on top of more dense water (Knauss, 1997). An example of a stably stratified water column is a lake in the summer. Normally, a pycnocline (density gradient) develops such that the water is much warmer (less dense) at the surface then at depth. In a stratified water column there is minimal mixing and the parcels remain vertically static for long periods (Knauss, 1997).

Unstable stratification defines a water body where a denser parcel overlies a less dense parcel (Knauss, 1997). This effect is uncommon but occurs at the poles when wind cools surface water to a lower temperature than at depth. Due to the change in potential energy the denser parcel attempts to sink and flip with the less dense water making it unstable (Knauss, 1997).

3.2.1 Andaman Sea Stratification

Applying these ideas to the Myanmar study area we expect to have stratification near river outflows. As seen in Fig. 2 the river often forms a plume of less dense water that overlies the denser salt water. Similarly, areas with a high potential for suspended sediment, fast current speeds near the bottom, have the possibility for developing very dense fluid mud bottom water. However, throughout most of the study area we would expect a well-mixed water column due to the turbulence created by strong tides, wind, and waves that mixes the water column and creates a more uniform density with depth.

3.3 Wind

As wind moves over the ocean's surface the friction creates a shear stress and in turn currents and waves develop. This effect can be seen when ripples form on the water's surface as a result of the wind blowing (Knauss, 1997). The stress is modeled by:

$$\vec{\tau_s} = \rho_a * C * \vec{U_{avg}} \tag{1}$$

Where $\vec{\tau_s}$ is the shear stress, ρ_a the air density, C the coefficient of drag, and U_{avg} the average wind speed (Wright, 1995).

Not limited to just the surface, the wind has an impact at depth, the shear forces the water to move fastest at the surface, and slows with depth to zero (See Fig. 8). The wind-driven flow takes place in a non-inertial frame.

The Coriolis force, present because of the earth's rotation, acts on the wind driven currents (Knauss, 1997). This creates a veering of the current with depth, known as an Ekman spiral displayed in Fig. 8. Since the magnitude of the Coriolis force is proportional to velocity, it effects the surface waters more so than waters deeper in the water column. This results in the net transport of water being directed 90 degrees to the right of the wind direction in the northern hemisphere, and 90 degrees to the left in the southern (Fig. 8) (Knauss, 1997). The veering of wind driven current directions via the Coriolis force drives three fascinating and vital processes: eddy's, upwelling. and downwelling.

3.4 Upwelling and Downwelling

Upwelling and downwelling result from wind blowing parallel to the shoreline. See Fig. 9 as the wind blows parallel up the shoreline the Ekman transport pushes water to pile up towards the shore. This creates a sea surface slope and pressure gradient such that the bottom water flows in a seaward direction (Knauss, 1997). As a result of conservation of mass, coastal waters sink (are down-welled) and are replaced by shoreward flowing waters. Wind blowing in the opposite direction pushes water offshore setting up the pressure gradient in the opposite direction, pulling surface water away from the shore. As a result of conservation of mass, new water is upwelled from the depths thus providing nutrient-rich waters to coastal ecosystems (Knauss, 1997).

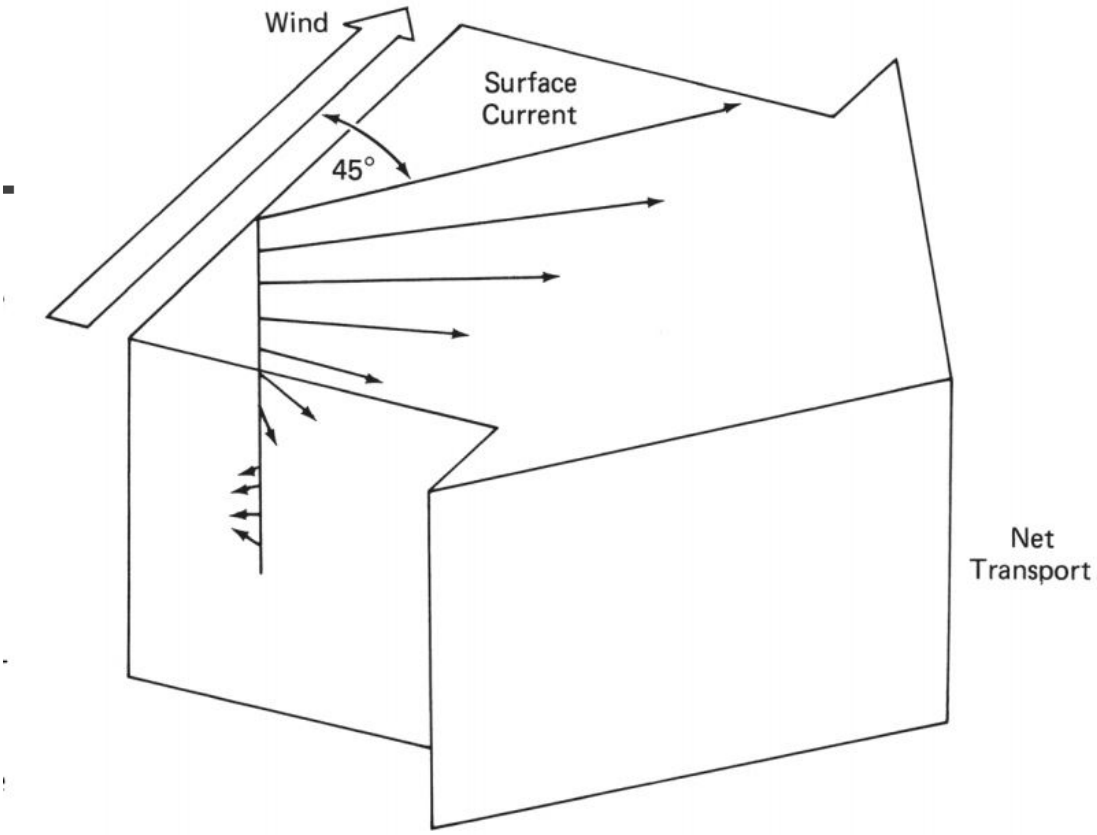

Figure 8: The Ekman spiral as a result of the Coriolis force and net transport for an example from the Northern Hemisphere. Surface currents are directed 45° to the right of the wind velocity. Ocean currents veer to the right with depth. In deep water, this sets up the water transport to be 90° to the right of the wind direction. Courtesy of Knauss (1997).

4 Motivation

Water column dynamics within the Northern Andaman Sea and coastal ocean offshore of the Ayeyarwady are not well understood. As mentioned above, theories exist that seasonal circulation imparts a bi-directional sediment transport pathway, where during NE monsoon conditions export suspended particles westward toward the Bay of Bengal, while under SW monsoon events the sediment would be pushed eastward into the Andaman Sea (Kuehl et al. (2019), Liu et al. (2020)). However, this theory was

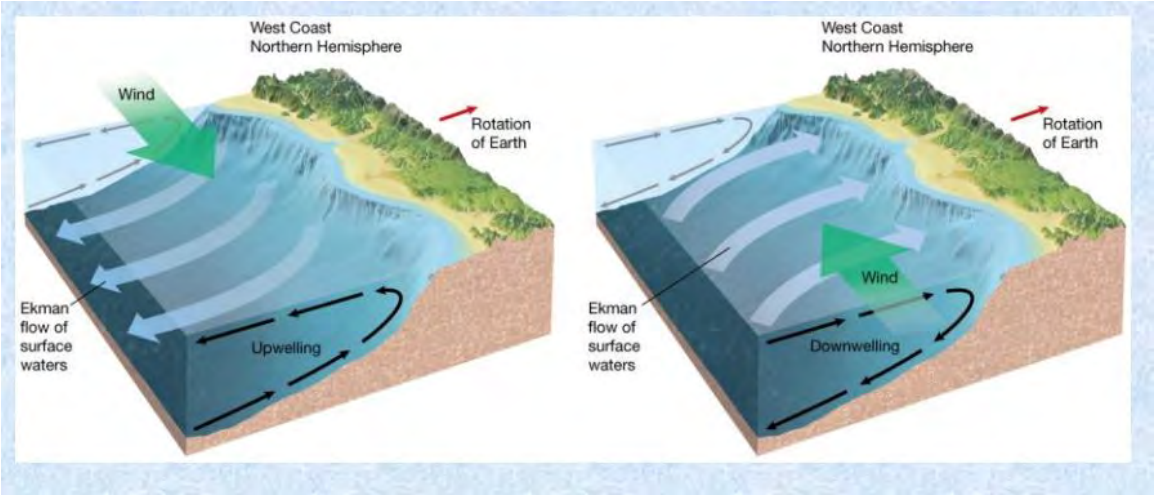

Figure 9: Displays the scenarios that create upwelling and downwelling along the shore. Courtesy of Buonaiuto (2018) .

based on surface current measurements from the 1960s studying ship tracks (Rodolfo, 1969). Velocities at depth are unmeasured and poorly understood. Furthermore, the Gulf of Martaban experiences highly energetic tides with amplitudes over 3 meters that drastically influence water column currents. Field data collected in December 2017 will be used in the future for developing numerical models to test the winter monsoon theory.

A recent numerical model that achieves 0.25 degree horizontal resolution over the study area display a perennial cyclonic eddy within the Gulf (Turner et al., 2019). Additionally, a numerical model that achieved higher horizontal resolution (0.1 degree) for the eastern Bay of Bengal predict that depth-averaged current flows fluctuate eastward and westward on a timescale of days (Chatterjee et al., 2017). Neither of these models include sediment transport (Turner et al. (2019) and Chatterjee et al. (2017)). Interestingly, while sediment researchers have often focused on the surface flow patterns (Kuehl et al. (2019),Liu et al. (2020), and Ramaswamy et al. (2004)), these numerical models show that in the northern Andaman Sea, currents in the deeper waters often flow in opposite directions to surface flows (Turner et al. (2019)

and Chatterjee et al. (2017)). Particularly interesting, they show very fast, northwestward currents at depth in the area south of the Ayeyarwady delta (Figure 12D of Turner et al. (2019); Figure 5 of Chatterjee et al. (2017)). Additionally, several CTD casts taken during the research cruise in 2017 showed strong stratification indicating a disconnect between flows at the surface and at depth (Kuehl et al., 2019). The lack of data on bottom boundary layer currents means that the flows that control sediment are unstudied and unknown. Observations of currents, turbidity, and turbulence at depth are needed to test numerical models and constrain sediment transport pathways. However, ADCP data was also collected during December 2017. The ADCP data measures, current velocity and provides a proxy for suspended sediment concentrations, thus recording information vital to the understanding of the sediment flows within the study area.

The ADCP data was analyzed to address specific research questions. First, the data was examined and processed for quality control. Then it was used to evaluate the questions: where and when in the study area are water speeds observed to be fast or slow? Additionally, what direction are the flows heading? What conditions and geographic locations have shear flows close to the bottom and what directions do the shear layers flow? And finally, what can we learn about suspended sediment patterns based on the ADCP observations?

5 Data Collection

During December 2017 a 2-week research cruise was conducted on the vessel the Sea Princess by scientists from the Virginia Institute of Marine Science, North Carolina State University, Mawlamyine University, and University of Yangon. During the cruise, which surveyed over 1500-km within the northern Andaman Sea and Bay of Bengal, an ADCP was mounted from the boat facing vertically downward toward the

ocean floor to record velocities within the water column (Fig. 11). Over 50 ADCP transects were recorded and they combine to geographically cover large portions of the northern Andaman Sea. The TDI (Teledyne Marine) ADCP was configured in mode 12 and recorded measurements of 255 consecutive vertical bins each with a thickness of 33 cm. Bottom tracking was used to determine the boat's relative speed to the seafloor, so that the current velocities could be reported relative to the seafloor. This assumes that a static seafloor can be sensed by the ADCP, and seems reasonable, due to the lack of indication of a moving bed. While on the cruise, 25-30 CTD (Conductivity Temperature and Depth) measurements were taken when the ship was anchored; the process involves lowering sensors that measure conductivity, temperature, and depth through the water column on a line from the surface to the bottom. A map of the selected ADCP transects after post processing quality control and associated, CTD, and tidal stations referenced for the research is located in Fig. 10.

6 Methods

Some initial background is necessary for understanding ADCP data. The ADCP uses acoustics theory to measure velocity in a fluid, relying on the presence of scattering particles in the fluid. Simply put, the ADCP emits known frequencies of acoustic energy as precisely timed "pings". It then records the reflected (backscattered) acoustic signal. Based on the time of return, and assumptions about the speed of sound in the fluid, the sensor can calculate the round-trip distance traveled by a signal. Subtle changes in the frequency of the returned signal result from a Doppler shift, which indicates that the reflecting particles were moving. The sensor uses these Doppler shifts to calculate the speed of the scattering particles, and assumes that the particles are moving with the ambient fluid. In this way, the sensor can provide a velocity

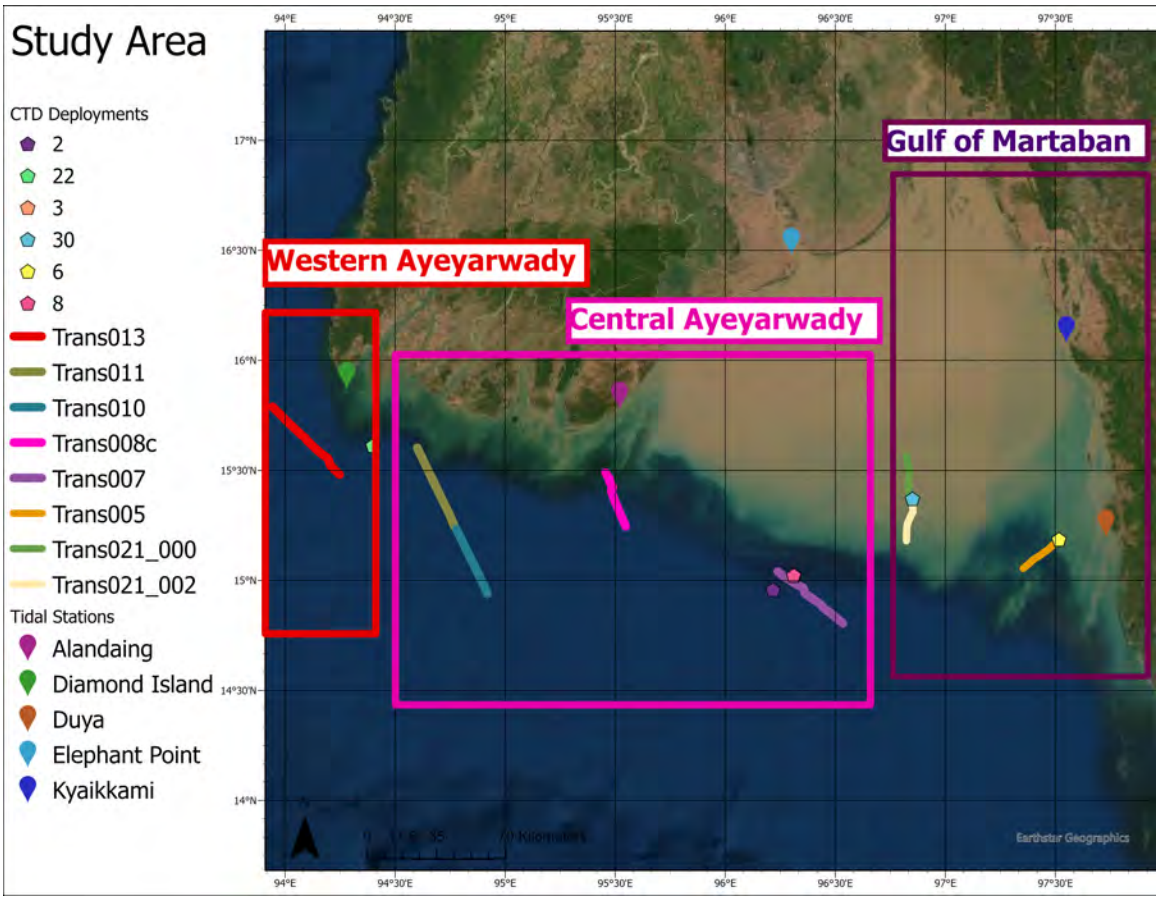

Figure 10: Displays the study area within the Andaman Sea. The map displays the ADCP transects with colored lines, tidal station locations are shown with different color drop pins, and the CTD locations are represented by pentagons and vary by color for each deployment.

profile; that is the measured velocity with distance from the sensor. By sending multiple beams of acoustics (Fig. 11), the three components of velocity can be calculated (i.e. eastward, northward, vertical). The backscatter intensity is the acoustic return energy measured in decibels. A high backscatter intensity reveals there were more particles to scatter and reflect the acoustic beam. These scattering particles can include phytoplankton, detritus, or suspended sediment. Therefore, more clear, clean water has a low backscatter, and turbid water with lots of sediment has a high backscatter.

The ADCP data was initially processed and quality controlled using the Winriver II software selecting bottom-tracking to calculate current velocities (Teledyne RD Instruments). Winriver II is a post-processing software provided by the manufacturer TRDI. The software was configured to track to the bottom and remove relative ship motion from the velocity data. Additionally, the software deletes bad data when the GPS signal or bottom detection is suspect, and determines flow velocities in the components of North and East via an inboard compass. The software can be configured to output backscatter (a measure of the energy of the returned beam), intensity, distance along transect, and more. Of the original transects, 8 were selected as having the most accurate data to be studied. The transects chosen are distributed through the study area. The backscatter data (used to visually determine different layers in the water column) was compared to CTD (Conductivity, Temperature, and Depth) sensor Voltage data to verify that the ADCP was working properly.

ADCP post-processing included removing transects where the GPS and bottom tracking data were unclear. Then a triangular smoothing of the velocity data was completed to filter spikes. To characterize tidal stage during the times that the ADCP data was obtained, tidal data from 5 different stations around Myanmar: Elephant Point, Duya, Yangon, Diamond Island, and Alandaing, was used depending on proximity to individual transects. In tidally dominated cases, the current directions were consistent with respect to the tides and conditions the cruise experienced.

7 Results

Interpreting the transects velocity and backscatter data was challenging. The ADCP profiles were taken from a moving vessel, each transect was several kilometers long, and required 4-12 hours to obtain. The large spatial and temporal lengths dictate that conditions while taking data were subject to change. Wind, currents, water depths,

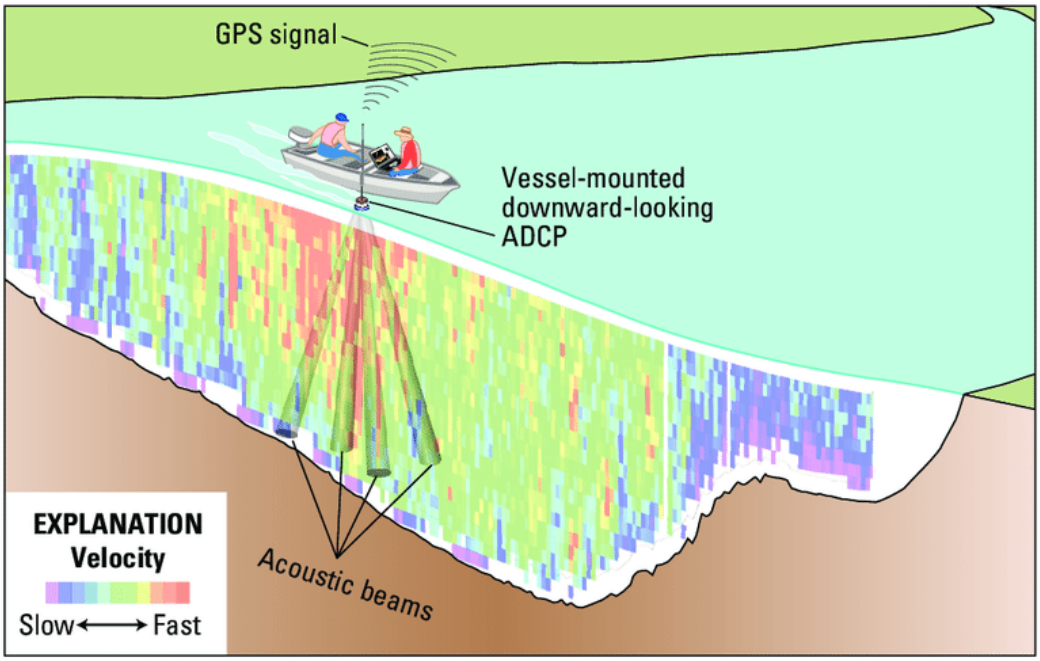

Figure 11: Displays bottom mount ADCP operation. In this scenario the ADCP is mounted to the bottom of the research vessel and records vertical transects of velocity as the boat was underway. The ADCP operates by sending acoustic energy in the form of 4 beams at an angle through the water column. The Doppler shift of the scattering particles is measured and then via geometry the current velocity in the north, east, and up directions are calculated. Courtesy of Mueller and Wagner (2013).

and tides all varied over the duration of each transect. Therefore, it was difficult to separate spatial from temporal effects. However, keeping this uncertainty in mind, we have characterized the conditions that generated each transect.

The ADCP transects were organized geographically into sections that displayed like characteristics as follows: Gulf of Martaban, Western Ayeyarwady Delta, and Central Ayeyarwady Delta. The Gulf of Martaban had fast energetic tides. The Western and Central Ayeyarwady had surface currents that were oriented toward the west. The Central Ayeyarwady Delta had apparent strong Northwestward bottom currents directed along bathymetric contours.

7.1 Gulf of Martaban

The Gulf of Martaban (Fig. 1, Fig. 10, and Fig. 6) has large tidal amplitudes that can exceed 2.5 meters, and large sediment inputs from the Ayeyarwady-Thanlwin river system. All three transects within the Gulf of Martaban were recorded during the spring/neap tidal transition or spring tides and generally occurred through slack velocity into flood tide (Fig. 12).

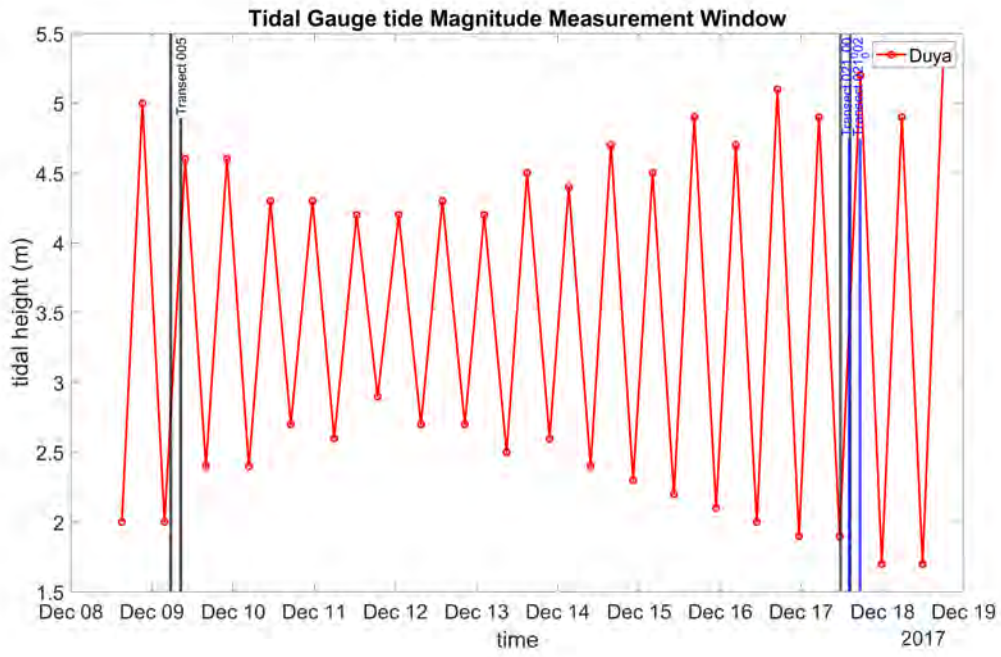

Figure 12: Displays the high and low tides for Duya, Myanmar during the 2017 research cruise. Duya is the closest available tidal station to the three transects taken in the Gulf of Martaban (Fig. 10 for locations). The horizontal axis displays time and the vertical axis displays tidal height. The vertical bars mark the duration of the three ADCP transects from the Gulf of Martaban: Transect 005 was obtained on December 9, and Transects 21-000 and 21-002 were obtained on December 17.

7.1.1 Transect 005

Transect 005 was recorded on December 9th, 2017 beginning at 05:34 UTC and finishing at 08:40 UTC. There are two possible interpretations for the data: one

considers temporal changes and the other spatial. The transect covered about 22 km on the eastern side of the Gulf of Martaban (Fig. 10). The boat traveled westward toward the middle of the Gulf of Martaban. The closest station to the transect is Duya (Fig. 12), and tidal conditions were shifting from the end of ebb, to low tide, to flood. Due to the strong tides within the Gulf of Martaban we would expect currents to be strongly interconnected to tidal processes.

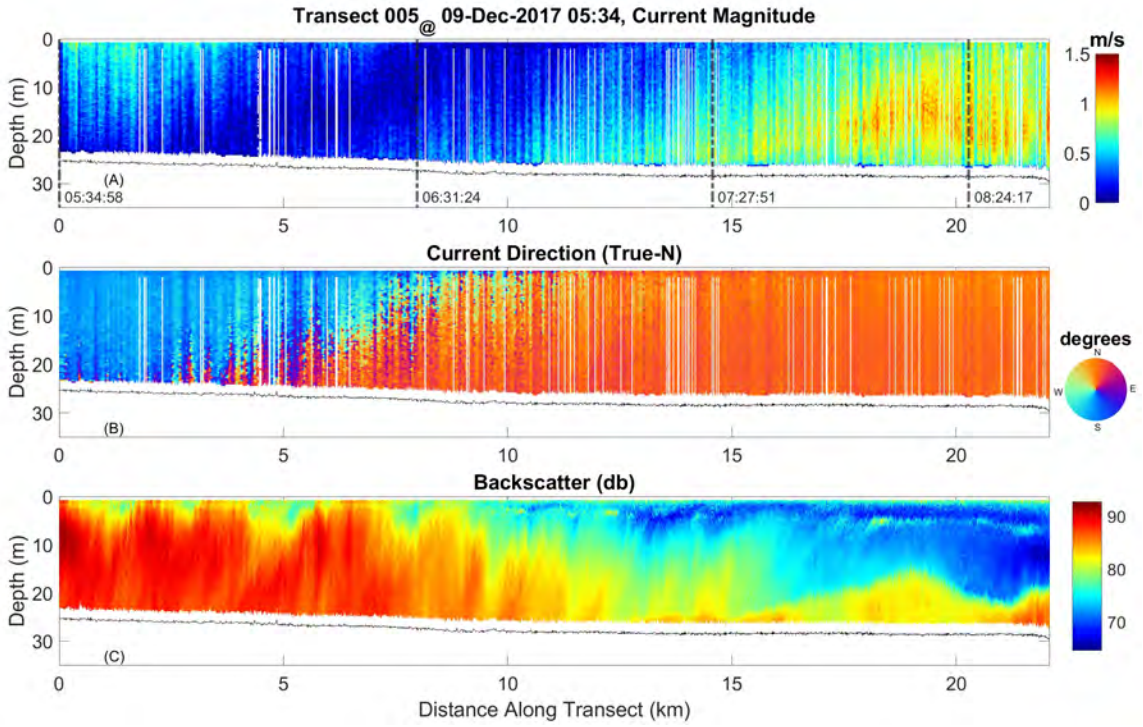

Figure 13: Displays the distance traveled on the horizontal axis, and water depth along the vertical axes. Top panel (A): water speed is displayed in the colorbar in m/s. Middle panel (B): direction toward which current flowed (see color wheel). Bottom panel (C): backscatter (a measure of the return energy in decibels) in the colorbar.

First, considering the temporal changes within speed and direction (Fig. 13 (A),(B)), there were high speeds that flowed southward which coincided with the ebb tide 0-5 km along the transect. Next, the speeds slowed to zero from 5-10 km along the transect during slack water at low tide. Finally, the current direction shifted northward

and speeds exceeded over 1 m/s during the flood tide from 10 km to the end.

Similarly, the backscatter followed the tidal cycle. Initially, from 0-5 km along the transect there was a high return at all depths suggesting high sediment concentrations throughout the water column (Fig. 13 (C)). As the boat proceeded westward and the water speeds slowed, corresponding to slack water at low tide, the layer of sediment started to settle through the water column. This can be seen as the high concentration (i.e. red in Fig. 13 (C)) settled downward and the upper water column cleared (green and blue in Fig. 13 (C)). The inverted backscatter structure continued from 5-13 km along the transect meaning there was lower particulate concentrations in the surface water and higher concentration towards the bottom. As the flood tide accelerated, a two-layer system developed from 20 km to the end of the transect (Fig. 13 (C)). There was evidence of re-suspended sediment in the bottom-most 5 meters of the water column (increase in return shown by yellow to red in the backscatter). At this time, the backscatter intensity showed a sharp gradient indicating the presence of a near-bed turbid layer overlain by the clear layer. The current velocity also showed speeds were slow within the turbid layer but reached very fast speeds (1.5 m/s) directly above the turbid layer. The resuspended sediment and any organic material associated with it has been eroded from the seafloor and reintroduced to the water column. This influenced water clarity and carbon availability for growth.

Next, we consider the data in terms of the spatial variations along the 22-km transect rather than temporal changes. At the beginning of the transect, in the shallower and more coastal site, sediment was present throughout the water column. When the boat traveled into deeper, more open water there was less sediment in the water column which is shown in the backscatter shift from red to blue. The two-layer system past 20 km remained and is shown in Fig. 13 that suggested tidal currents heavily influence sediment pathways.

Both temporal and geographic interpretations included high initial sediment concentrations, the settling of suspended sediment and carbon, and development of a two-layer system that was re-suspending sediment and carbon off the bottom reintroducing it to likely oxygenated waters, where geochemical reactions might fuel biological growth.

7.1.2 Transect 21: 000 and 002

Transect 021 was divided into two parts, named 21-000 and 21-002. Transect 21-000 was started on December 17, at 11:39 UTC and was completed at 14:20 UTC. The boat headed south within the middle of the Gulf of Martaban for about 18 km (Fig. 10). The geographic location of the transect suggested that water currents would be heavily dependent on tides and highly energetic as tidal amplitude in this location exceeded 2 m (Fig. 12).

There was about a 40 minute phase lag in tides from the transect location to the Duya tidal station based on a numerical model developed by Matthew Fair (VIMS) that included sea surface height calculations. At Duya the tides were initially ebbing, then slowed as low tide was reached, and then flood tide commenced (Fig. 12).

First, we consider the role of the tides in the current's speed and direction (Fig. 14). The transect was recorded during the end of the ebb to low tide. During the ebb, from 0 to 10 km along the transect, there were slow current speeds toward the south (Fig. 14). About midway through, starting at about 10 km along the transect, current speeds slowed to zero when low tide was reached. At the very end of the transect, around 17 km, flood tide commenced and current speeds accelerated to 0.5 m/s in a northward direction (Fig. 14).

At the beginning of the transect (0 to 8 km) there were 3 distinct backscatter layers (Fig. 14). The layering had higher backscatter in the surface waters overlying

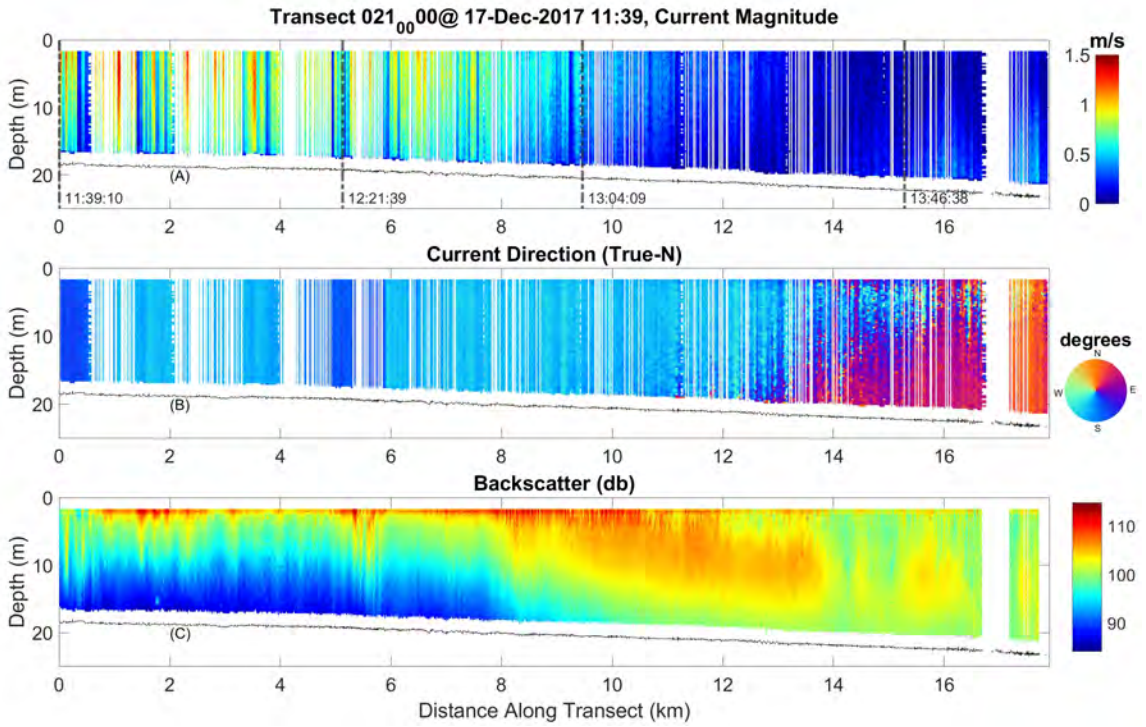

Figure 14: Displays the distance traveled on the horizontal axis, and water depth along the vertical axes. Top panel (A): water speed is displayed in the colorbar in m/s. Middle panel (B): direction toward which current flowed (see color wheel). Bottom panel (C): backscatter (a measure of the return energy in decibels) in the colorbar.

lower returns, indicating that the flow was carrying more turbid water toward a less turbid location. Past 8 km currents speeds slowed and sediment began to settle. The settling occurred since there was no longer fast-moving water to hold the sediment particles in suspension in the water column. The sinkage continued from about 8 km to 14 km and was shown by the red layer descending in the water column (Fig. 14 (C)). As current speeds increased from 14-18 km along the transect, the flood tide commenced and gained strength (Fig. 12 and Fig. 14). During flood tide, the water column became better mixed as evidenced by the reduced vertical variation in the backscatter.

Considering Transect 21-000 from a spatial perspective the tidally influenced cur-

rents remained the same as above, but the backscatter was interpreted differently. As the boat headed south away from the Ayeyarwady Delta, into more open water, the higher turbidity (higher backscatter) at the surface sunk deeper into the water column (due to its greater density). This continued past 8 km until it settled to the bottom (Fig. 14 (C)).

Transect 21-002 was recorded immediately following 21-000 with the boat traveling in the same direction. Data collection began on December 17, at 14:29 UTC and ended at 17:26 UTC that same day. While underway the boat traveled about 21 km in a southerly direction (Fig. 10). The tides were flooding during this time (Fig. 12). Much like transect 21-000 we would expect water speeds to depend on the tides due to the $>$ 2 m tidal amplitude.

Shifting to Fig. 15, current speeds were initially slow but increased to over 1.2 m/s by about 8 km along the transect. The acceleration coincided with tides transitioning from slack water to flood tide during this time. Water direction was northward throughout the transect.

The backscatter (Fig. 15) was initially well mixed which shows continuity with the end of transect 21-000. As the tidal velocities increased during the flood from around 6 km along the ship track there were two distinct layers with higher backscatter in the bottom most 5-20 meters. The presence of the 2-layer flow, suggested the water was pulling mud and sediment off the bottom and transporting it northward. Furthermore, sediment concentrations during the flood tide seemed smaller than during the ebb tide, based on comparing the backscatter intensity during these times (Fig. 14 and Fig. 15). During the flood tide, the bottom layer had a backscatter of 100 db whereas the surface layer had a backscatter of 80 db at their interface. The higher backscatter in the bottom layer suggests that there was more sediment in the bottom layer than the surface, and because currents were slow within this turbid layer, the

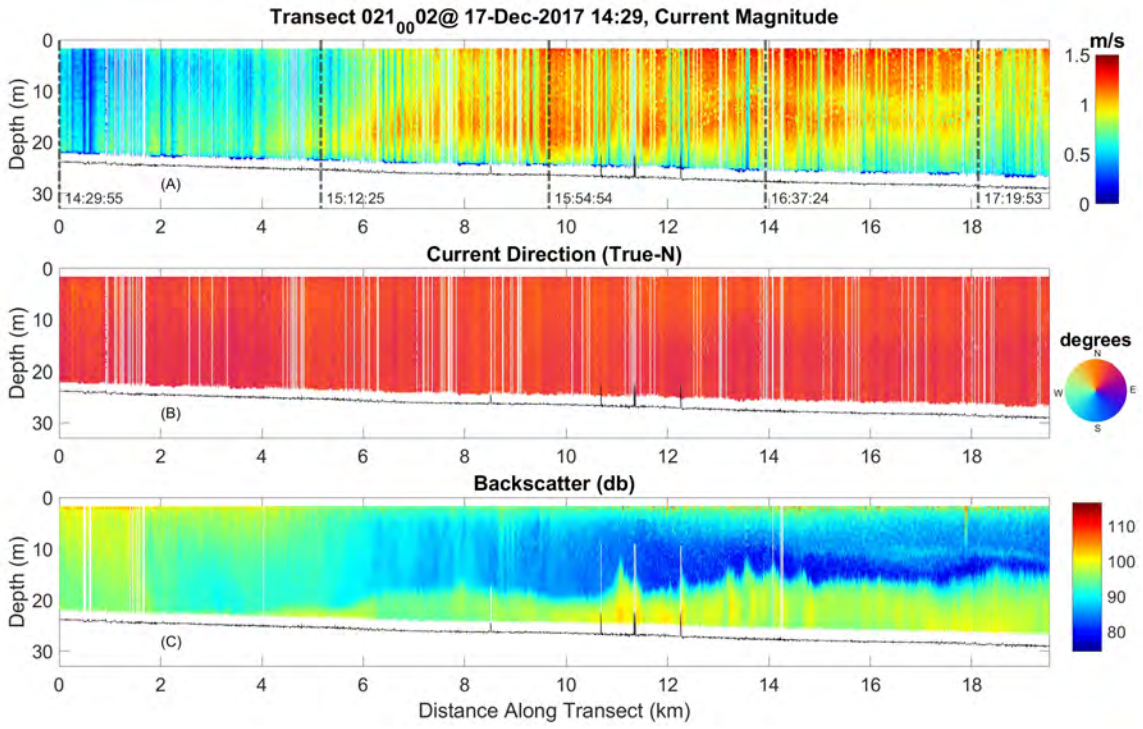

Figure 15: Displays the distance traveled on the horizontal axis, and water depth along the vertical axes. Top panel (A): water speed is displayed in the colorbar in m/s. Middle panel (B): direction toward which current flowed (see color wheel). Bottom panel (C): backscatter (a measure of the return energy in decibels) in the colorbar.

suspended sediments may have been a fluid mud. Currents get fast enough within the area to resuspend sediment and likely play a large role in carbon and sediment dynamics.

Next, we consider transect 21-002 from a geographic perspective. The boat continued to travel south with this transect. As it headed into deeper water, turbidity reduced at the surface as shown by the decrease in backscatter (Fig. 15). The increasing return in the near-bed flows of the deeper portion of the transect resulted from resuspension by the tides, but the resuspended sediment was trapped in the bottom layer, being overlain by the clearer surface water.

The combination of transects 21-000 and 21-002 is powerful since together they

covered an entire tidal cycle from ebb conditions through low tide and into flood. In general, over that cycle, there were faster currents when the tides were accelerating through flood tide, and slower currents at low and high tides. During both ebb and flood tidal conditions current speeds exceeded 1 m/s. Both the tidal and geographical interpretation of the data supported that the backscatter indicated more sediment in the water during the ebb tide of transect 21-000 while the boat was closer to the delta. This was expected since the ebb would be pulling turbid estuarine water seaward into the ocean. Finally, during the strong tidal flows in the flood tidal phase, a two-layer flow developed with a possible fluid mud layer on the bottom.

7.1.3 Gulf of Martaban in Summary

The transects selected within the Gulf of Martaban, all taken during the Spring tide, had highly energetic tides, very fast current speeds, and were directionally dependent on the tidal phase. The area was characterized by sediment flows southward during ebb, and possible re-suspension off the bottom at shallow depths during flood.

7.2 Central Ayeyarwady Delta

Four transects: 07, 08c, 010, and 011 were selected from the Central Ayeyarwady Delta region. The transects were recorded during the neap tidal phase between December 10, 2017 and December 12, 2017 (Fig. 16). Compared to the Gulf of Martaban the area experienced lower tidal amplitudes, only about ±0.5 m (Fig. 16).

7.2.1 Transect 007

Transect 007 was recorded on December 10-11, 2017 from 21:24 UTC on the 10th to 02:45 UTC on December 11th. The transect was recorded while the tides were ebbing (Fig. 16). The boat traveled offshore of the eastern edge of the Ayeyarwady delta and over the mouth of the Martaban Depression and Canyon for about 30 km (Fig. 10).

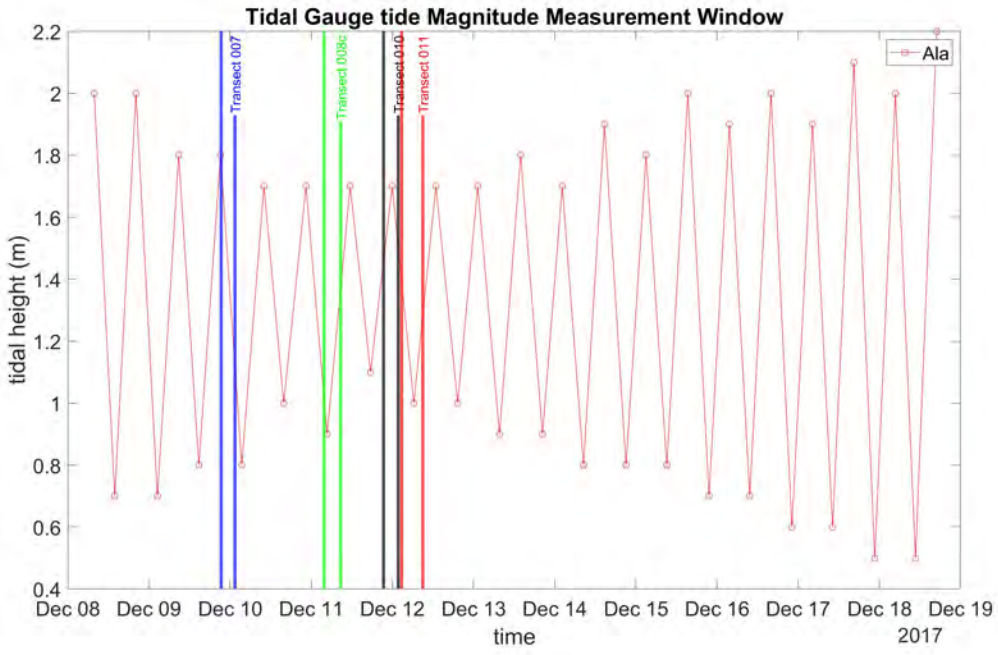

Figure 16: Displays the nearest tidal stations to transects 07, 08c, 010, and 011 (Fig. 10) for locations. The closest station to the transects was Alandaing. Time is on the horizontal axis and the vertical axis displays tidal height.

While traversing this region, the boat crossed a steeply-sloped bottom contour where there may be unpredictable currents as the steep walls of the Martaban Depression can constrict flows of water.

The measured speed and direction profiles were intriguing. Current speeds were close zero in the upper 35 meters of the transect from beginning to end (Fig. 17). Underneath that calm layer, below 35 meters, from 0 to 35 km along the transect, there was a highly energetic shear layer with speeds above 2 m/s (Fig. 17 (A)). The shear layer flowed in a northwestward direction, parallel to the bathymetric contours. These fast currents may have developed from deep upwelling. Numerical models indicate that fast northwestward currents with speeds around 1 – 2 m/s may be formed at depth in this area ((Chatterjee et al., 2017) Figure: 4). However, without confirmation the veracity of these current speeds is unclear.

Within the backscatter data there was a clear, higher return layer at around 20 m in depth along the entire length of the transect (Fig. 17 (C)). Underneath that layer there was a less defined layer of higher return about 20 m above the bottom until about 30 km along the transect (Fig. 17 (C)). That higher return layer at depth aligned with the fast-moving bottom water indicating that it had a higher concentration of particles than the upper water column (Fig. 17 (C)). These differences may result from cold salty water being pulled into the Martaban Depression.

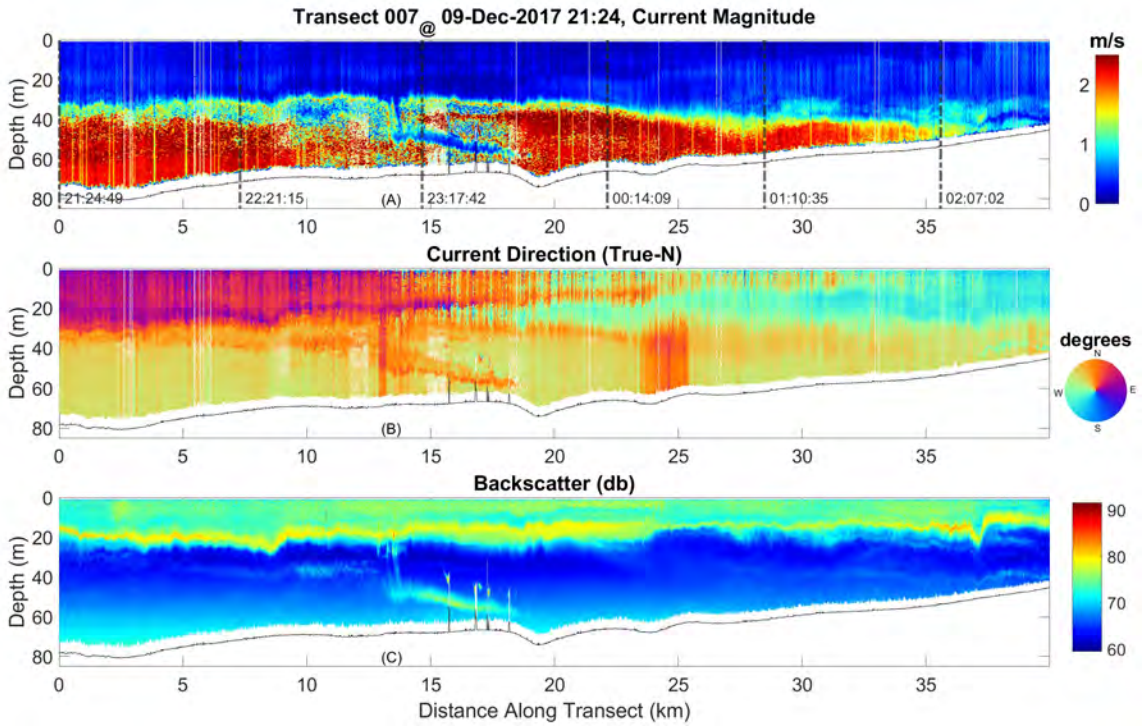

Figure 17: Displays the distance traveled on the horizontal axis, and water depth along the vertical axes. Top panel (A): water speed is displayed in the colorbar in m/s. Middle panel (B): direction toward which current flowed (see color wheel). Bottom panel (C): backscatter (a measure of the return energy in decibels) in the colorbar.

7.2.2 Transect 008

Transect 008 was located close to the central Ayeyarwady Delta (Fig. 10). The transect measurement began on December 11, 2017 at 04:48 UTC and the boat headed northwestward toward the shore until 08:51 UTC that morning. The transect traversed about 30 km in water depths that ranged from about 48 m to 10 m. Tidal conditions were flooding and the transect began at low tide, but similar to transect 007 the tides were not expected to be a major factor as tidal energy is low here (Fig. 16).

Throughout the transect, currents were moderate. The maximum speed reached was about 0.5 m/s and flowed in a westward direction (Fig. 18 (A),(B)). Within the first 5 km of the transect there was a pocket of fast-moving bottom water that flowed in the northwestward direction (Fig. 18). This bottom water flow pattern could be an extension of currents recorded in transect 007.

In the deeper part of the transect, around 5 – 15 km, the backscatter intensity was at its highest in the middle of the water column. In the shallower portion of the transect, 15 – 30 km, the backscatter increased in intensity as depth decreased and was highest near the bed. This indicated the presence of near-bed, resuspended coastal sediments closer to the Delta (Fig. 18 (C)).

7.2.3 Transect 10

Transect 10 was located offshore, south of the Ayeyarwady Delta. The transect was recorded from 21:27 UTC on December 11th to 01:53 UTC December 12th for about 3 hours 30 minutes total (Fig. 21). The boat traveled in a northwest direction, and traversed about 35 km in water depths ranging from about 45 to 35 m (Fig. 19). The tides at stations on the Delta: Alandaing and Diamond Island (Fig. 10), were flooding, reached high tide, and began to ebb while the transect was recorded.

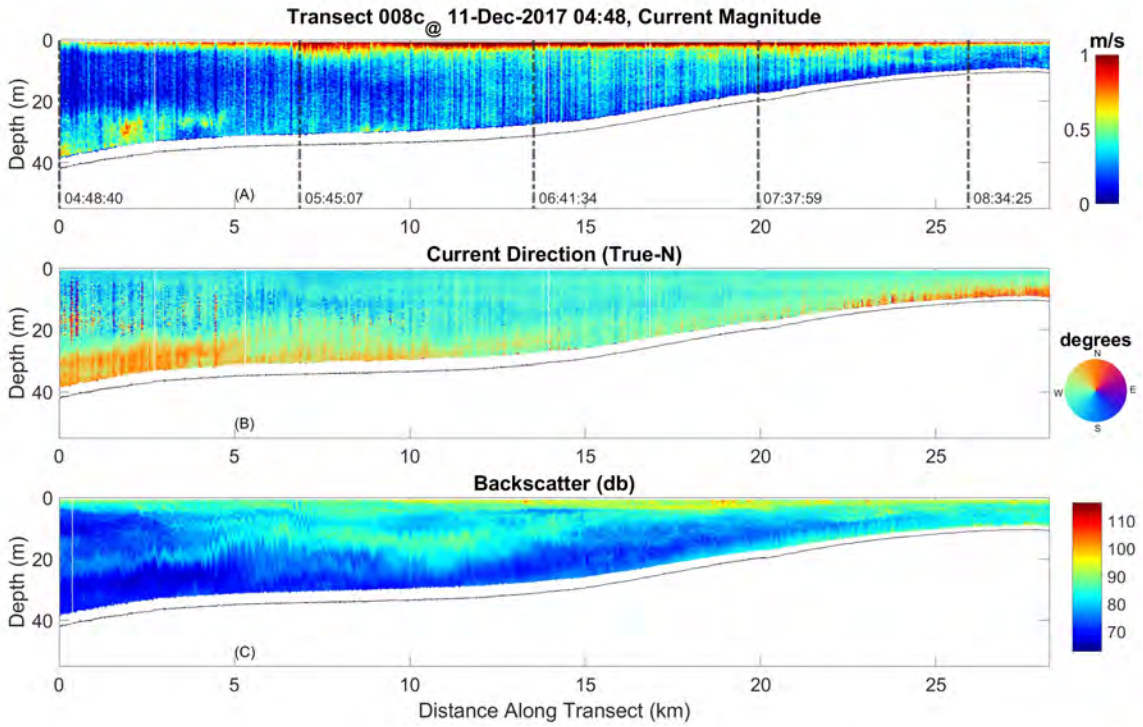

Figure 18: Displays the distance traveled on the horizontal axis, and water depth along the vertical axes. Top panel (A): water speed is displayed in the colorbar in m/s. Middle panel (B): direction toward which current flowed (see color wheel). Bottom panel (C): backscatter (a measure of the return energy in decibels) in the colorbar.

The speeds were moderate (<0.2 m/s). Below 40 meters depth, a fast shear layer appeared to be present in the bottom 5-10 m very near the sea floor across the entire length of the transect (Fig. 19 (A)). The shear layer appeared to have intense speeds exceeding 2 m/s flowing in a northwestward direction similar to transect 007. Such intense speeds at depth were surprising. The shear layer was also defined in the backscatter by a distinct gradient at about 40 m depth through the entire length of the transect. Potential mechanisms for these fast bottom boundary layer currents included near-bed upwelling water, but further confirmation of these currents would be needed to validate them.

In the middle depths there were scattered flows at about 0.5 m/s but all were in

the northwestward direction. The fact that the current direction did not shift over tidal timescales suggests that the tidal energy was much lower here than in the Gulf.

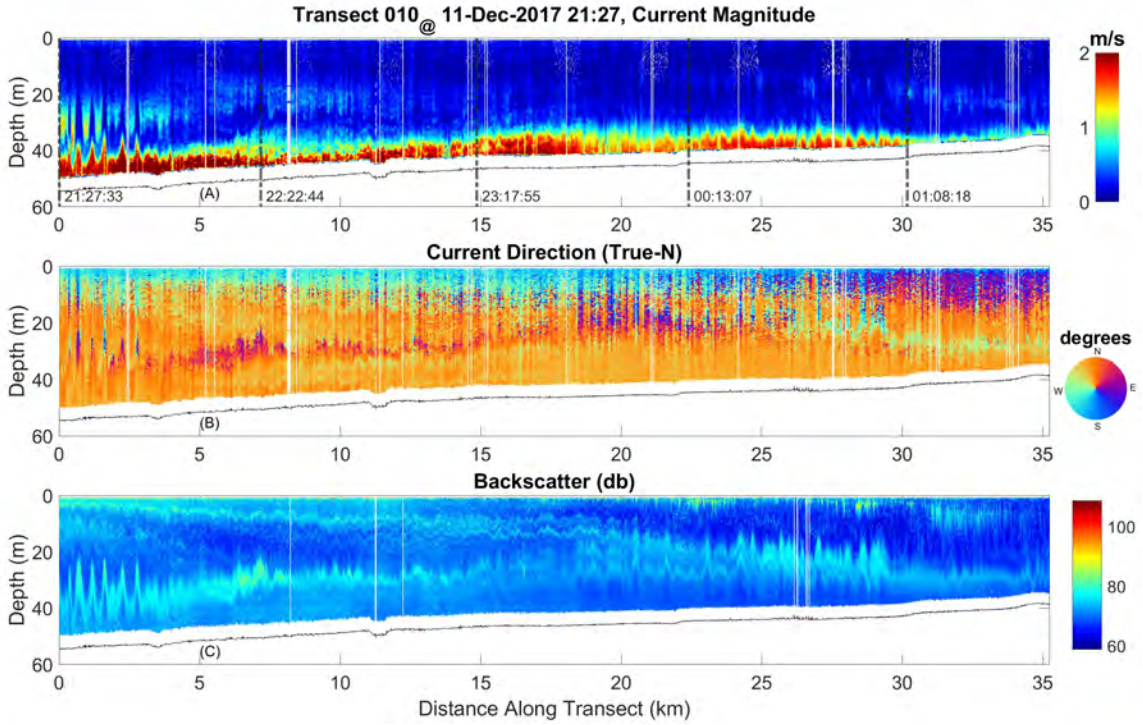

Figure 19: Displays the distance traveled on the horizontal axis, and water depth along the vertical axes. Top panel (A): water speed is displayed in the colorbar in m/s. Middle panel (B): direction toward which current flowed (see color wheel). Bottom panel (C): backscatter (a measure of the return energy in decibels) in the colorbar.

7.2.4 Transect 11

Transect 11 was a continuation of transect 10, where the boat traveled in a northwestward direction from 02:46 UTC on December 12th to 09:00 UTC that same day for a total time of about 4 hours and 16 minutes underway. This transect traversed 35 km, from water depths of 60 m to 50 m. Tides at the Alandaing and Diamond Island stations (Fig. 10) were ebbing, reached low tide, and began to flood during this time (Fig. 21). However, similar to transect 10, the tidal energy was low and did

not seem to greatly influence currents.

As a continuation of transect 10, transect 11 was expected to have similar features and characteristics at adjacent points in the two transects for quality control. Examining the end of transect 10 (Fig. 19 (A)) and beginning of 11 (Fig. 20 (B)) the speeds, directions, and backscatter profile all aligned at similar depths. This showed continuity between the two transects. Specifically, both transects had a distinct backscatter layer at 30 m, and modest currents speeds at the surface and in the middle water column.

Transect 11 showed similar characteristics to transect 10 in that they both had moderate speeds in the upper water column. The near-bed shear layer seen in transect 11 is not as apparent in transect 10, but there is a pocket of fast-moving northwestward direction water in the middle of the transect from about 20 to 30 km in distance covered (Fig. 20 A). Similar to the layer in transect 10, this layer was also moving in the northwestward direction at speed exceeding 1 m/s. This could be an extension of the fast-moving bottom water seen in transect 007.

The backscatter return was low and consistent in the first kilometer, suggesting well mixed water. A driver for this could have been wave and wind action or low sediment concentrations at that time. However, as the boat traveled closer to the delta the backscatter increased (Fig. 20 (C)). That increase in backscatter could have been due to the muddy, less dense fresher water flowing out of the river offshore of the western Ayeyarwady. The high backscatter return surface layer existed from 1 km to the end, but increased in thickness close to shore. Theoretically, as the boat got closer to the shore, the freshwater plume would be less dilute as it had not been exposed to much mixing and dilution with saltier sea water. A clear, stratified water column developed from 2.5 km to the end of the transect where higher backscatter (more sediment was present at the surface) and a second layer underneath it registered with

less backscatter and sediment (Fig. 20 (C)). Under those two layers, was a layer that had even weaker return, which we interpret as clearer water underneath the more turbid river outflow (Fig. 20 (C)).

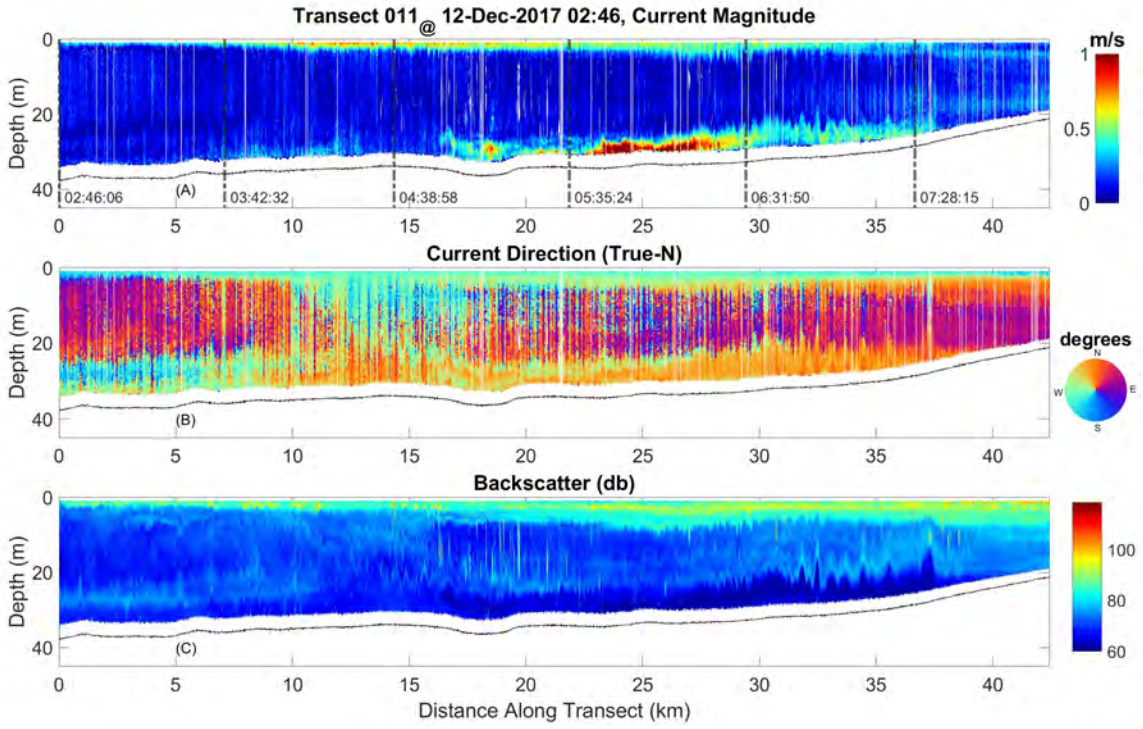

Figure 20: Displays the distance traveled on the horizontal axis, and water depth along the vertical axes. Top panel (A): water speed is displayed in the colorbar in m/s. Middle panel (B): direction toward which current flowed (see color wheel). Bottom panel (C): backscatter (a measure of the return energy in decibels) in the colorbar.

7.2.5 Central Ayeyarwady in Summary

The area within the middle of the Ayeyarwady delta appeared to have strong north-westward bottom currents, which could be a result of deep upwelling, and a general westward flow throughout the water column. The general westward flow aligned with the conceptual model presented by Kuehl et al. (2019). The velocities here were in general lower than those seen in the Gulf of Martaban, both because this area has

lower tides, and this area was sampled during neap tidal conditions. For most of the water columns sampled, currents were on the order of 10's of cm/s, directed toward the west. The exception to this were the apparent fast bottom layer of currents that were seen along the bottoms of transects 007 and 010, which had apparent currents in excess of 1.5 m/s directed northwestward.

7.3 Western Ayeyarwady Delta

One transect was obtained in the western Ayeyarwady region between December 11-13, 2017. Tidal records from the nearby Alaindang and Diamond Island stations showed that this was during neap tides (Fig. 21). In this location the tidal amplitude ranges from ±1 m during spring tides to only about ±0.5 m during neap conditions.

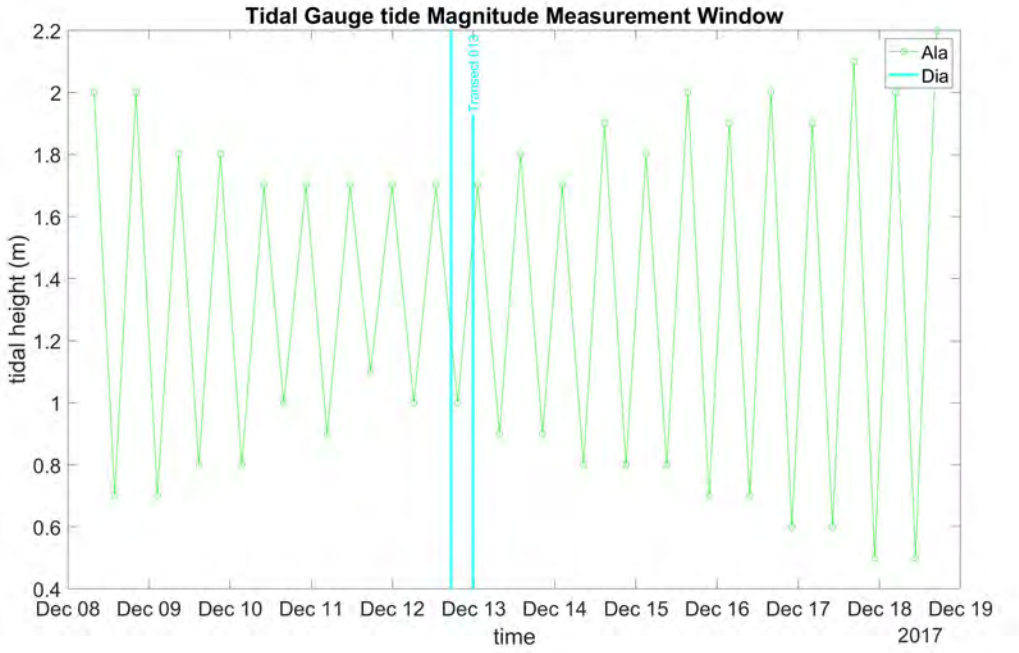

Figure 21: Displays the water levels for the nearest tidal station to transect 13 (Fig. 10). The closest stations to transects are Alandaing and Diamond Island. The time is on the horizontal axis and the vertical axis displays tidal height.

7.3.1 Transect 13

Transect 13 was recorded from Dec. 12 at 17:23 UTC to Dec. 13 at 01:00 UTC (Fig. 21). The boat traveled offshore of the western edge of the Ayeyarwady Delta and headed toward the northwest, roughly following an along-shore direction (Fig. 10). This transect traversed a 52 km – long path, in water depths from 40 to 70 m. The tidal energy was low and currents were expected to be driven by monsoonal winds and regional oceanographic circulation pushing water in a westward direction.

Current speeds were about 0.5 m/s and slower than those observed in the Gulf of Martaban. Currents flowed in a northwestward direction at all depths from 0 to about 2 km along the transect (Fig. 22 (A),(B)). Currents did shift to northeastward from about 2 to 3 km, this shift could be due to the tides flooding northward or the Bay of Bengal influencing dynamics (Fig. 22 (A,B)). From 3 km to the end of the transect, the currents flowed in a northwestward direction (Fig. 22 (A,B)). The insensitivity of the current direction with changes in tide reaffirmed the lack of tidal influence.

The backscatter had higher return in the lower part of the water column for X $<$ 10km, then shifted to be in the upper water column for X $>$ 30 km (Fig. 22 (C)).

7.3.2 Western Ayeyarwady Delta in Summary

When compared with the Gulf of Martaban the tidal energy was drastically less in the western Ayeyarwady region. The change in sea surface height at each tidal station was only about 0.5 meters, in contrast to over 5 meters seen at tidal stations in the Gulf of Martaban (Fig. 21). This decrease in tidal energy means that the tides were much less important for water column characteristics.

The transect featured in the Western Ayeyarwady Delta section measured currents that flowed in the northwestward direction.The prevailing northwest flow cor-

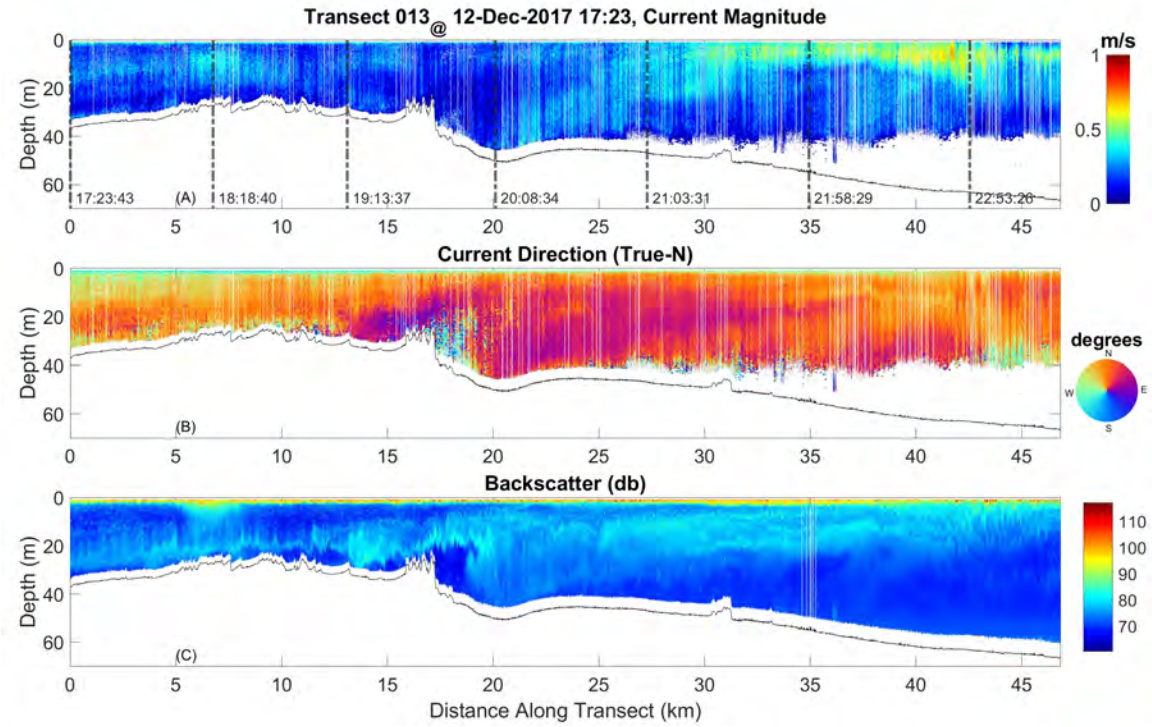

Figure 22: Displays the distance traveled on the horizontal axis, and water depth along the vertical axes. Top panel (A): water speed is displayed in the colorbar in m/s. Middle panel (B): direction toward which current flowed (see color wheel). Bottom panel (C): backscatter (a measure of the return energy in decibels) in the colorbar.

responded to the ideas presented by (Kuehl et al., 2019) from previous data. This pattern was consistent with the westward monsoonal winds pushing the water, and the response to larger scale oceanographic circulation.

8 Synthesis

Conditions within the study area varied spatially and temporally while the transects were being recorded. Overall, the research cruise covered 2-weeks that included the transition from spring tides to neap tide, and then the beginning of spring tides. A total of about 250 km of ADCP transects were analyzed, which accounted for about 28 hours of sampling. The spatial extent covered an area from the eastern Gulf of

Martaban to the western Ayeyarwardy Delta; and sampled water depths from as shallow as 10 m to as deep as 80 m. More detailed information of the summary below can be found above in Section 7.

Of the regions sampled, the Gulf of Martaban (Section 7.1) experienced the highest tidal energies and the speed and direction of currents were heavily dependent on tidal phase (Fig. 23). Additionally, the transects within the area were recorded during times in the spring/neap cycle when the tidal force was relatively strong. Water speeds commonly exceeded 2 m/s at peak flood tide and flowed in a northward direction. During ebb tides the currents shifted southward and attained similar speeds. During ebb the backscatter was either evenly spread through the water column or restricted to a surface plume. This indicated that sediment was being advected, or transported, out of the muddy Gulf of Martaban. During slack, two of the transects showed sediment settling out of the water column. During a flood tide two of the transects (Transect 005 and 21-002) showed highest backscatter in the bottom boundary layer, indicating the presence of resuspended material. The ADCP also recorded low currents in this turbid layer, though currents were fast above it. This may indicate the existence of fluid muds.

In the Central Ayeyarwady (Section 7.2) tides were much smaller and as such had much less influence on the water velocity compared to those observed in the Gulf of Martaban. Additionally, the transects were recorded during the neap tidal phase when tidal energy was at its lowest. Within that section, water speeds in the upper water column were on average less than 0.2 m/s and trended in a northwestward direction. In the bottom half of the water column (Fig. 23) there was evidence of fast-moving shear layers. These fast shear layers could have been plumes produced by upwelling of deep water, funnelled through the Martaban Canyon and Depression. In transect 007 water speeds were over 2 m/s deep in the water column along the steep

upper walls at the head of the Martaban Depression. These highly energetic speeds were located in an unpredictable steep-walled topography that is over 500 m tall. Without further confirmation, we must maintain some skepticism of these currents, but it is worth noting that this apparent feature was seen in other transects, and also that a recently published numerical model shows some similar currents (Figures 4 and 6 (Chatterjee et al., 2017)) produced by water upwelled from the deep Andaman Sea. In the upper half of the water column velocities were much slower but also tended to be directed toward the northwest. Possible remnants of this fast-moving bottom water were found in two transects: transect 010 and transect 011. Both of these transects featured speeds that exceeded 1 m/s in a bottom shear layer heading in a northwestward direction. In addition, both of these transects had much slower speeds (< 0.5 m/s) in surface waters. In the Central Ayeyarwady region, water velocities did not flow with the tides to the extent of those speeds in the Gulf of Martaban.

The single transect analyzed from the Western Ayeyarwady (Section 7.3) was also recorded during the neap tidal phase, and showed similar features to those from the central area. Currents in this transect (Transect 013) were slower < 0.6 m/s in the surface waters, and trended in a general northwestward direction (Fig. 23).

9 Conclusions

Conditions within the study area (Fig. 10) were highly variable in both space and time. Over the 2-week research cruise collecting ADCP measurements, water column speeds and structure varied from near 0 m/s to 2 m/s depending on location, tidal phase, and other forcings. From east to west, the tidal forces decreased in magnitude and influence. Understanding the tides within the Gulf of Martaban is vital for water currents, sediment deposition, and resuspension. However, in the Central and Western regions tides were not major forces in the water speed and directions.

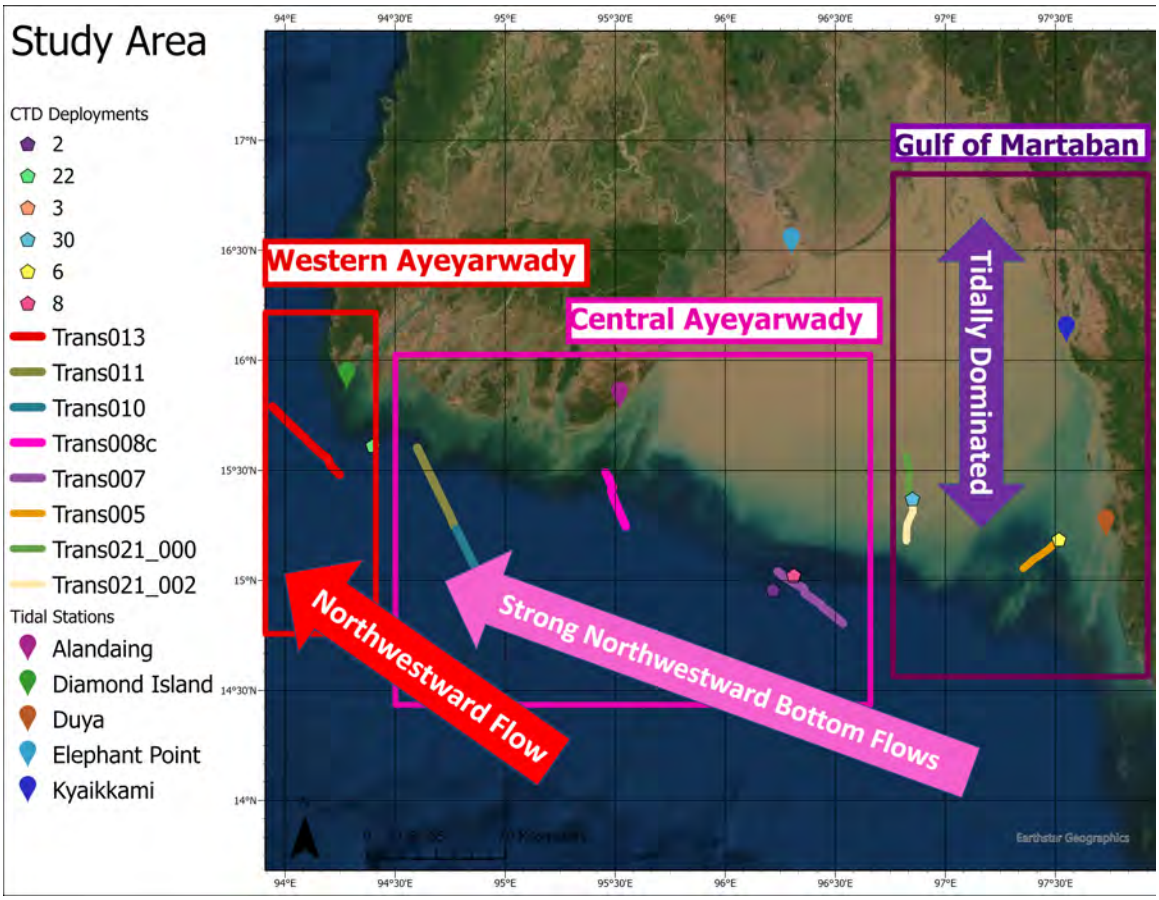

Figure 23: Displays the study area within the northern Andaman Sea showing the location of the ADCP transects with colored lines, tidal station locations are shown with different color drop pins, and the CTD locations are represented by pentagons and vary by color for each deployment. The arrows summarize the general flows characteristics found in each zone.

The Gulf of Martaban and neighboring Ayeyarwady Delta is a highly dynamic and energetic environment, and conditions vary over time and space. Although there is a general understanding of circulation based on observations of surface currents and numerical ocean models, this ADCP data represents a unique set of observed currents and backscatter intensity. The data suggested that within hours, water characteristics can shift drastically away from the mean, and also that conditions in the bottom boundary layer may differ drastically from surface conditions. With this knowledge, for increased accuracy, more work should be done to investigate the perturbations that

the ADCP recorded: fast moving bottom shear layers, over 2 m/s tidal currents, and varied sediment concentrations. ADCP data within the western and central regions of the northern Andaman Sea indicated the presense of deep shear layers of fast-moving water that could possibly be upwelled deep Andaman Sea water, or residuals from benthic storms (energetic unpredictable bottom events). More data needs to be collected of these events to further characterize them as either unusual episodes, common features, or ascertain whether they are artifacts of the data. If the currents are in fact real, they would significantly alter current dynamics, numerical models, and sediment transport for this region. It is necessary to understand the highly complex, chaotic system to better understand current flows that control sediment and carbon transport. With that powerful information global climate studies and our understanding of global warming will vastly increase.

References

Bauer, J. E., Cai, W.-J., Raymond, P. A., Bianchi, T. S., Hopkinson, C. S., Regnier, P. A. G. 2013. The changing carbon cycle of the coastal ocean. Nature (London), 504(7478):61–70.

Bianchi, T. S., Allison, M. A., Cai, W. J. 2013. Biogeochemical dynamics at major river-coastal interfaces : Linkages with global change. Cambridge University Press, New York.

Bird, M., Robinson, R., Win Oo, N., Maung Aye, M., Lu, X., Higgitt, D., Swe, A., Tun, T., Lhaing Win, S., Sandar Aye, K., Mi Mi Win, K., Hoey, T. 2008. A preliminary estimate of organic carbon transport by the Ayeyarwady (Irrawaddy) and Thanlwin (Salween) Rivers of Myanmar. Quaternary International, 186(1):113 – 122. Larger Asian rivers and their interactions with estuaries and coasts.

Buonaiuto, F. 2018. Chapter7. University Lecture. Http://www.geo.hunter.cuny.edu/$\sim$ $fbuon/GEOL\_180/GEOL180\_S2018\_Ch7.pdf$.

Chatterjee, A., Shankar, D., McCreary, J. P., Vinayachandran, P. N., Mukherjee, A. 2017. Dynamics of Andaman Sea circulation and its role in connecting the equatorial Indian Ocean to the Bay of Bengal. Journal of Geophysical Research: Oceans, 122(4):3200–3218.

Grill, G., Lehner, B., Thieme, M., et al. 2019. Mapping the World's Free-Flowing Rivers. Nature, 569(221):215–221.

Hedley, P. J., Bird, M. I., Robinson, R. A. J. 2010. Evolution of the Irrawaddy delta region since 1850. The Geographical Journal, 176(2):138–149.

Hossain, M. S., Sarker, S., Sharifuzzaman, S., Chowdhury, S. R. 2020. Primary Productivity Connects Hilsa Fishery in the Bay of Bengal. Scientific Reports, 10(1):1–16.

Knauss, J. 1997. Introduction to Physical Oceanography. Prentice Hall.

Kuehl, S. A., Williams, J., Liu, J. P., Harris, C., Aung, D. W., Tarpley, D., Goodwyn, M., Aye, Y. Y. 2019. Sediment dispersal and accumulation off the Ayeyarwady delta – Tectonic and oceanographic controls. Marine Geology, 417:106000.

Liu, J. P., Kuehl, S. A., Pierce, A. C., Williams, J., Blair, N. E., Harris, C., Aung, D. W., Aye, Y. Y. 2020. Fate of Ayeyarwady and Thanlwin Rivers Sediments in the Andaman Sea and Bay of Bengal. Marine Geology, 423:106137.

Meybeck, M., Laroche, L., Dürr, H., Syvitski, J. 2003. Global variability of daily total suspended solids and their fluxes in rivers. Global and Planetary Change, 39(1):65 – 93. The supply of flux of sediment along hydrological pathways: Anthropogenic influences at the global scale.

Mueller, D., Wagner, C. 2013. Measuring discharge with acoustic Doppler current profilers from a moving boat. Measuring Discharge with Acoustic Doppler Current Profilers from A Moving Boat.

Ramaswamy, V., Rao, P., Rao, K., Thwin, S., Rao, N., Raiker, V. 2004. Tidal influence on suspended sediment distribution and dispersal in the northern Andaman Sea and Gulf of Martaban. Marine geology, 208(1):33–42.

Robinson, R., Bird, M., Win Oo, N., Hoey, T., Aye, M. M., Higgitt, D., Lu, X., Swe, A., Tun, T. 2007. The Irrawaddy River Sediment Flux to the Indian Ocean: The Original Nineteenth-Century Data Revisited. The Journal of Geology, 115.

Rodolfo, K. S. 1969. Sediments of the Andaman basin, northeastern Indian Ocean. Marine Geology, 7(5):371–402.

Syvitski, J. P., Saito, Y. 2007. Morphodynamics of deltas under the influence of humans. Global and Planetary Change, 57(3):261 – 282.

Taylor, J., Taylor, S. 2005. Classical Mechanics. University Science Books.

Teledyne RD Instruments. WinRiver II.

Turner, A. G., Bhat, G. S., Martin, G. M., Parker, et al. 2019. Interaction of convective organization with monsoon precipitation, atmosphere, surface and sea: The 2016 INCOMPASS field campaign in India. Quarterly journal of the Royal Meteorological Society, 146(731):2828–2852.

Wright, L. D. 1995. Morphodynamics of inner continental shelves. Marine science series. CRC Press, Boca Raton.

Zaw, Z. L., Wittenberg, H. 2015. Hydrology and flood probability of the monsoon-dominated Chindwin River in northern Myanmar. Journal of Water and Climate Change, 6(1):144–160.